ELSEVIER

Carbohydrate Polymers 40 (1999) 29–47

Carbohydrate Polymers

Glass transition and physical properties of polyol-plasticised pullulan–starch blends at low moisture

C.G. Biliaderis*, A. Lazaridou, I. Arvanitoyannis

Laboratory of Food Chemistry and Biochemistry, Department of Food Science and Technology, School of Agriculture, Aristotle University, P.O. Box 256, Thessaloniki, Greece 540 06

Received 16 September 1998; received in revised form 5 January 1999; accepted 9 February 1999

Abstract

The effects of water and polyols, at low weight fractions, on water sorption behaviour, thermal and mechanical properties, and gas permeability of blends of pullulan and gelatinised corn starch (ps), prepared by either hot pressing or casting aqueous solutions, were studied. Incorporation of sorbitol or xylose in the ps blends resulted in lower equilibrium moisture contents in the low to medium a_w range, and much higher moisture contents at $a_w > 0.75$; the Guggenheim–Anderson–DeBoer isotherm model adequately described the sorption data up to the a_w of 0.9. Water and polyols exerted a strong plasticising action, lowering the T_g of the blends and allowing enthalpy relaxation events to occur during aging of the amorphous specimens. At the low polyol levels examined (10 and 20% dry basis), a single glass transition temperature for the polymeric constituents was identified in all samples by DSC and DMTA; apparent activation energies of 226–296 kJ mol^{-1} for the α-relaxation were estimated from multifrequency mechanical measurements. Large deformation mechanical tests demonstrated sharp decreases in Young's moduli with increasing levels of polyol and water, typical of the glass–rubber transition of amorphous polymers; the relationship of flexural modulus and moisture content was quantified using the Fermi's model. The relationship between maximum stress (σ_{max}) and water content showed an increase in stiffness of the blends from 7 to 11% moisture, and a strong softening effect when the water content exceeded this range. The Arrhenius plots of O_2 and CO_2 permeability data showed distinct changes in slope in the glass transition region of the blends. Analysis of viscoelastic data with the time–temperature superposition principle and treatment of gas permeability data with the Williams–Landel–Ferry equation suggested that application of this model is meaningful if the coefficients, C_1 and C_2, are allowed to vary instead of assuming their 'universal' values.

Keywords: Pullulan; Gelatinised corn starch; Sorbitol; Xylose; Glass transition temperature; Oxygen and carbon dioxide permeability

1. Introduction

There has been increased interest in the structural and property changes that occur in glassy biopolymers and biopolymer blends as a result of physical aging or plasticisation effects brought about by solvents and other small molecular weight co-solutes. This is due to the sustained incursion of biodegradable polymeric materials into demanding new applications, particularly in the area of thermoplastic materials (e.g. starch-based plastics) or coating films, as well as the need to provide a better insight into the functional role of food constituents in formulated products (e.g. extrusion and baked cereal products). The structure–property relationship of hydrated biopolymers and their broader implications on processing and product quality can be better understood within the theoretical framework of glass transition, commonly used in polymer science (Fennema, 1996; Karel, Buera, & Roos, 1993; Levine & Slade, 1988a, 1992; Slade & Levine, 1991). Supercooled polymer melts exhibit rapid decrease in molecular mobility which parallels a sudden increase in viscosity as the glass transition temperature of the polymer is approached. The glass transition (α-relaxation, reflecting primarily motions of fairly long chain segments in the amorphous domains of a polymer) denotes a threshold of precipitous change in some material properties, e.g. modulus. Changes in the mechanical properties of a polymer around T_g are of a major practical interest as glasses have high elastic moduli (Young's or shear moduli), i.e. they are hard and brittle. By raising the temperature a glassy material enters the rubbery domain with a concomitant drop ($\approx 10^3$ times) in the elastic moduli (Sperling, 1986). The glassy state is frequently described as a state of relatively high stability as diffusion-controlled physical or chemical processes practically cease and only localised small-amplitude

---

* Corresponding author. Tel.: +30-31-998-785; fax: +30-31-998-789.
E-mail address: biliader@agro.auth.gr (C.G. Biliaderis)

0144-8617/99/$ - see front matter
PII: S0144-8617(99)00026-0

motions (rotations and vibrations) continue to occur. As a result of the latter small amplitude movements (mainly involving atoms, groups of atoms, or polymer side chains), the so-called γ- and β-relaxations, local mobility exists in the glassy state leading to limited structural reorganisations. It should be noted, however, that the physics of polymers in the glassy state is far from being well understood despite the extensive research for the last 30 years (Ibar, 1997; Keinath, Miller, & Rieke, 1987; Mansfield, 1993); e.g. the existence of local structure (chain morphology in the solid state) and even the origin (intra- vs. inter-molecular effects) of the two most fundamental and recognised transitions of glassy polymers, the T_g and T_β (β-relaxation) are still topics of debate among scientists in this field.

Many studies on low-moisture systems have shown that water exerts a strong plasticising action in hydrophilic polymers, causing a large depression of their glass transition temperature, T_g. On a molecular level, moisture-induced plasticisation of a polymer leads to increased intermolecular distances (free-volume), decreased local viscosity and increased back-bone chain segmental mobility (Slade & Levine, 1991). Practically, the addition of low molecular weight plasticisers to an amorphous matrix has the same effect as increased temperature on molecular mobility. The relationships between T_g and moisture content may be shown on simplified state diagrams which describe the concentration dependence of T_g and the relationships between ice formation and solute concentration at low temperatures (Levine & Slade, 1988b; Roos & Karel, 1991). State diagrams have become popular among food scientists (Karel et al., 1993; Roos & Karel, 1991; Roos, 1995; Roos, Karel, & Kokini, 1996; Slade & Levine, 1993) as they are useful to characterise the physical state of food solids and to demonstrate food quality modifying events, e.g. crystallisation of sugars or starch, stickiness and flow behaviour of food powders, structure collapse phenomena and crispness loss in freeze dried or extruded cereal products.

Many investigations have been conducted during the last decade on thermal events and mechanical properties of food biopolymers as affected by water or low molecular weight solute plasticisation (Appelqvist, Cooke, Gidley, & Lane, 1993; Biliaderis, Page, Maurice, & Juliano, 1986; Bizot, Le Bail, Leroux, Davy, Roger, & Buleon, 1997; Cherian, Gennadios, Weller, & Chinachoti, 1995; Donald, Warburton, & Smith, 1993; Forssell, Mikkila, Moates, & Parker, 1997; Gontard & Ring, 1996; Hoseney, Zeleznak, & Lai, 1986; Kalichevsky, Jaroszkiewicz, Ablett, Blanshard, & Lillford, 1992a; Kalichevsky, Jaroszkiewicz, & Blanshard, 1992b,c, 1993a; Kalichevsky, Blanshard, & Tokarczuk, 1993b; Kalichevsky & Blanshard, 1993; Nicholls, Appelqvist, Davies, Ingman, & Lillford, 1995; Noel, Parker, Ring, & Tatham, 1995; Shogren, 1992; Soest, Hulleman, Wit, & Vliegenthart, 1996a; Vodovotz & Chinachoti, 1996; Zeleznak & Hoseney, 1987). As there is interest in the behaviour of actual food products in the glassy state, there has been also a growth of studies on the thermal and mechanical behaviours of biopolymer blends (Arvanitoyannis, Psomiadou, & Nakayama, 1996; Arvanitoyannis & Biliaderis, 1998; Psomiadou, Arvanitoyannis, & Yamamoto, 1996; Kalichevsky & Blanshard, 1992) and cereal-based products (Buera, Jouppila, Roos, & Chirife, 1998; Georget & Smith, 1995; Hallberg & Chinachoti, 1992; Kaletunc & Breslauer, 1993; Le Meste, Huang, Panama, Anderson, & Lentz, 1992; Le Meste, Roudant, & Davidou, 1996; Livings, Breach, Donald, & Smith, 1997; Roudaut, 1998). Investigations of blends or composites of biopolymers alone or with synthetic polymers is a promising area of material science as it may lead to new materials with improved functional properties and biodegradability at relatively low cost.

The present study was undertaken to examine the effect of plasticisation by water and polyols (sorbitol and xylose) on the thermal, mechanical and gas permeability (GP) properties of starch–pullulan (1:1) blends. Although the potential of using starch (as native or chemically modified) and pullulan (a microbial polysaccharide) in plastics or as coating and film forming materials has been long recognised (Whistler, BeMiller, & Paschall, 1984; Wurzburg, 1986; Yuen, 1974), their behaviour in multicomponent systems has not been widely explored for compatibility with other components, phase behaviour, mechanical properties, gas permeation and water adsorption. Thus, a further aim of this work was to provide such information for blends of these two α-D-glucans prepared by either compression moulding or casting from aqueous solutions.

2. Experimental

2.1. Materials and sample preparation

Granular corn starch (amylose content 26%) was rendered amorphous by gelatinising 30% w/w starch slurries in a roller drier (one process) at 140°C (roller-drier speed 10 rpm; pressure 32 psi ≈ 221 kPa; gap 1 mm; diameter 165 mm; width 150 mm). Pullulan was purchased from Hayashibara Biochem. Lab. Inc., Okayama, Japan. Sorbitol and xylose (analytically pure) were obtained from Wako Pure Chemical Industries Ltd. (Japan). Inorganic salts (reagent grade) used for adjusting the relative humidity were from Merck (Darmstadt, Germany).

Pullulan, gelatinised corn starch and polyols were mixed in a dry form at the appropriate weight ratio. Preparation of thick specimens (1.0–1.5 mm), suitable for thermal analysis and mechanical tests (bending mode), was carried out by spraying the dry powder mix with water (30–35% w/w), conditioning the hydrated blends for 4 h and hot pressing at 115°C for 8 min and later at 125–130°C for 10–12 min at ~ 2.5 MPa. Hydration of these materials at various levels of moisture was achieved by either conditioning in different relative humidity chambers (saturated salt solutions) or exposing the samples to 100% relative humidity for different periods of time. The preparation of composite films (0.1 ± 0.05 mm) for gas and water vapour permeability (WVP) tests was carried out by solution casting (60°C) over plexiglas (methyl methacrylate) plates, followed by slow drying at 30–35°C for several days.

2.2. Sorption isotherms

Portions of approximately 300 mg of dehydrated films (dried under vacuum at 60°C for 24 h) were spread in weighing dishes and kept over saturated salt solutions in small desiccators under vacuum. Several salt solutions were used to achieve various relative humidities: LiCl, CH_3COOK, $MgCl_2 \times 6H_2O$, K_2CO_3, $Mg(NO_3)_2 \times 6H_2O$, $NaNO_2$, NaCl, KCl and KNO_3 which give a_w values (25°C) of 0.11, 0.23, 0.33, 0.43, 0.53, 0.64, 0.75, 0.84 and 0.94, respectively (Rockland, 1960; Greenspan, 1977; Labuza, Kaanane, & Chen, 1985). The saturated salt solutions were kept for two days before use at the aforementioned temperatures. The closed desiccators with the samples were stored in water baths (PolyScience, Niles, IL) at 25°C. The moisture content of the samples, after reaching equilibrium (at least one week), was determined by drying at 130°C for 1 h. Six determinations were made on all equilibrium moisture contents for each sample formulation. The a_w moisture data were used to construct sorption isotherms. The data were fitted to the Brunauer–Emmett–Teller (BET) (Brunauer, Emmett, & Teller, 1938) or the Guggenheim–Anderson–DeBoer (GAB) (van den Berg & Bruin, 1981) sorption-isotherm models.

The BET model is described by the equation

$$a_w/(1 - a_w)m = 1/m_m K + a_w(K - 1)/m_m K$$

where m_m is the BET monolayer value, and K is a constant. The constants m_m and K were calculated from the linear regression of the experimental data in a specified range of a_w values.

The three-parameter GAB isotherm model is given by the equation

$$m/m_m = CKa_w/(1 - Ka_w)(1 - Ka_w + CKa_w)$$

where C is a constant. For data-fitting purposes this model can be transformed into a second-order polynomial

$$a_w/m = \alpha(a_w^2) + \beta a_w + \gamma$$

from which the constants C and K and the m_m can be calculated by the following equations (Bizot, 1983):

$$m_m = \sqrt{-1/(4\alpha\gamma - \beta^2)},$$

$$K = [\beta - (1/m_m)]/ - 2\gamma \text{ and } C = 1/(m_m \gamma K)$$

2.3. X-ray diffraction analysis

The wide angle X-ray diffraction analysis was performed on composite films and powdered specimen after equilibration in a specified relative humidity environment. The samples were attached to specifically made plexiglas holders and examined with a Philips X-ray generator PW 1830 equipped with a graphite-crystal monochromator and a vertical goniometer PW 1820. The operating conditions for the refractometer were: copper K_a radiation, voltage 40 kV, amperage 30 mA, sampling interval time 0.4 s.

2.4. Differential scanning calorimetry

Differential scanning calorimetry (DSC) was carried out using a PL DSC-Gold calorimeter (Polymer Labs. Ltd, Epsom, UK). Small amounts (20–30 mg) of materials were placed onto aluminium pans and conditioned at various relative humidities (saturated salt solutions or water) in desiccators at 25°C. The samples were then hermetically sealed and analysed under continuous flow of dry N_2 gas at a heating rate of 5°C min^{-1}. Temperature calibration was made with cyclohexane, dodecane and octane, whereas heat flow calibration was made by reference to the known melting enthalpy of indium and gallium (purity 99.99 %) from Goodfellows Metals. For constructing the state diagrams, the T_gs were determined as the middle points of the transitions from the second heating scan after heating the sample at a temperature 10–15°C above its T_g and quenching it with liquid nitrogen. Data analysis to fit experimental values of T_g to the empirical Gordon–Taylor (G–T) equation (Gordon & Taylor, 1952) was performed using the TableCurve™ software (Jandel Scientific), a non-linear least-squares curve fitting package:

$$T_g = \frac{w_1 T_{g_1} + kw_2 T_{g_2}}{w_1 + kw_2}$$

where w_1 and w_2 are the respective weight fractions of the polymer blend and water, T_{g_1} is the T_g of the composite polymer matrix, T_{g_2} is the T_g of the amorphous water, and k is a constant related to the strength of polymer–diluent interaction (the larger the k, the greater the plasticisation effect). The k constant is equivalent to the ratio of the heat capacity changes at T_g of the pure diluent and the polymer matrix, $\Delta Cp_2/ \Delta Cp_1$, as it appears in the Couchman–Karasz (C–K) equation (Couchman & Karasz, 1978). A T_g of -138°C was used for water (Sugisaki, Suga, & Seki, 1968).

2.5. Dynamic mechanical thermal analysis

The dynamic mechanical thermal analysis (DMTA) Mark III analyser (Polymer Labs, Loughborough, UK) was employed on hot pressed thick specimens ($\sim 2.2 \times 0.5 \times 0.2$ cm^3), conditioned at various levels of moisture content, in the single cantilever bending mode at frequencies of 1, 3 and 10 Hz and a strain × 2, corresponding to a maximum displacement of 32 μm. The analyser compares the stress and strain signals and resolves the strain into the in-phase (storage) and out-of-phase (loss) components from which storage or elastic (E') and loss (E'') moduli as well as the $\tan \delta = E''/E'$ are obtained as a function of temperature.

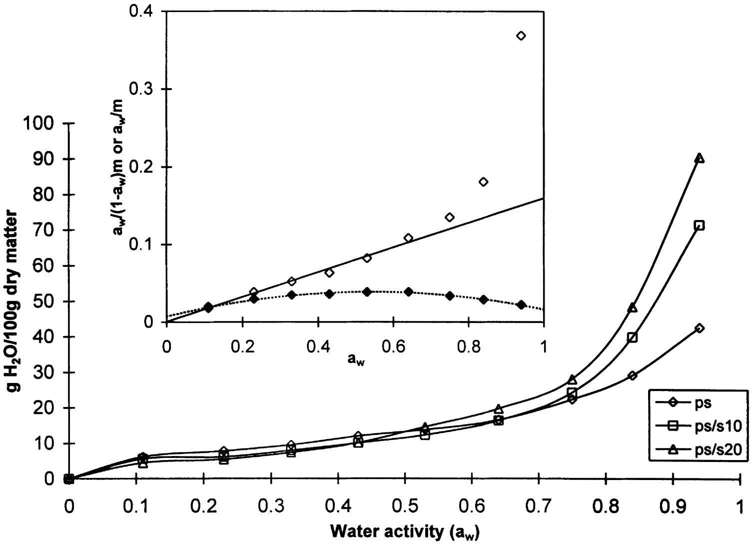

Fig. 1. Sorption isotherms of pullulan/gelatinised corn starch blends with and without sorbitol (10, 20% d.b.) at 25°C; inset shows the BET (solid line) and GAB (dotted line) adsorption models for the ps sample.

The standard heating rate used was 2°C min^{-1}. For polymeric materials a drop in storage modulus and a peak in tan δ are used as indicators of a glass transition; the tan δ peak is normally found at a temperature higher than the onset or the midpoint temperature of the modulus (E') drop; the peak temperature of tan δ increases with increasing frequency, as expected for any thermally activated relaxation process. For some specimens, measurements at a variety of frequencies (0.3, 1, 2, 3, 5, 10, 20, 30 and 50 Hz) were performed at several temperature steps (isothermally, using increments of 5°C between 30 and 90°C). The data (E') collected from these tests were used to generate master curves by employing the time/temperature superposition principle (Ferry, 1980). The moisture content of samples used for thermal analysis was determined by drying at 130°C for 1 h.

2.6. Large deformation mechanical tests

2.6.1. Three-point bending test

Hot pressed samples were cut with a scalpel or scissors into bars ($\backsim 7.0 \times 1.1 \times 0.2\ \text{cm}^3$) and after conditioning at various moisture contents they were analysed with a TA-XT2i instrument (Stable Micro Systems, Godalming, Surrey, UK) at 25°C. The Young's or flexural modulus (E) was calculated from the initial slope of the force vs. deformation curve according to the equation (van Krevelen, 1990):

$$E = (FL^3)/4bd^3y$$

where F is the load at a displacement y of the sample bar (taken from the linear portion of the stress–strain curve), L, the span width between the supporting bars, and b and d, the width and thickness of the bar. Each of the reported moduli values represents an average of at least six samples similarly conditioned to a certain moisture level. With the flexural moduli values expressed in a logarithmic scale, the following Fermi's empirical model (Peleg, 1996a; Harris & Peleg, 1996) was applied to fit the sigmoidal curves of E vs.m

$$E(m) = (E_0 - E_r)/\{1 + \exp[(m - m_c)/b]\} + E_r$$

where $E(m)$ is the magnitude of modulus; m the moisture content of the sample; E_0 the initial modulus (dry or glassy state); m_c the characteristic water content where $E(m) = E_0/2$; b is a constant describing the steepness of the modulus drop around the m_c; and E_r the residual magnitude of modulus after the transition.

2.6.2. Tensile test

Hot pressed sample bars ($3.5 \times 0.6 \times 0.2\ \text{cm}^3$), after their conditioning at various moisture contents, were tested with a TA-XT2i instrument according to the ASTM (1989). Measurement conditions and calculations of tensile strength, tensile modulus and percentage elongation were made as described elsewhere (Arvanitoyannis & Psomiadou, 1994). Moisture content determination of samples used for large deformation mechanical testing was by drying the samples at 105°C to a constant weight.

From the stress–strain curves of both flexural and tensile tests, a maximum stress ($\sigma_{\max}$) value was also obtained.

2.7. Gas and water vapour permeability tests

The measurements of GP through solution-casted films were carried out using a Davenport apparatus connected to an IBM/PC in accordance with the ASTM D1434-66 (ASTM, 1966). Permeability P is the product of solubility (S) and diffusivity (D) of a gas in a polymer. The formula for

Table 1
Estimated parameters for water sorption data of pullulan/corn starch blends (25°C) using the BET and GAB isotherm models

Sample	BET (a_w: 0.11 − 0.64) m_m (g of H_2O/100 g)	K	r^2 ($n = 6$)	GAB (a_w: 0.11 − 0.94) m_m (g of H_2O/100 g)	K	C	r^2 ($n = 9$)
ps	6.3	399.5	0.98	7.7	0.88	20.6	0.98
ps/s10	6.0	19.7	0.99	6.0	0.99	20.3	0.96
ps/s20	7.6	5.2	0.92	7.0	1.01	6.9	0.91
ps/x10	7.8	41.2	0.99	7.8	0.97	55.0	0.95
ps/x20	9.2	182.0	0.99	9.9	0.96	20.2	0.95

the determination of the gas diffusion constant is as follows:

$$D = \frac{d^2}{6\theta}$$

where d is the thickness of the film and θ is the time lag of permeation; film thickness was measured with a micrometer at five or six locations of the film. The lagθ is related to the time required by the gas to establish an equilibrium in an originally gas-free film; i.e. achieve steady-state conditions. The extrapolation of the pressure increase-time curve to the zero axis produces the time lagθ. The quantity of gas, Q, passing through the film is directly proportional to the difference in pressure exerted by the gas on each side of the film ($p_1 - p_2$), to the film area exposed, A, to the permeation time, t, and is inversely proportional to film thickness, x. This relationship could be expressed with the equation

$$Q = \frac{PAt(p_1 - p_2)}{x}$$

where P, having a constant value for a specific combination of gas and polymer at a given temperature, is known as the “transmission factor” or permeability factor, constant or coefficient.

WVP measurements were carried out at 25°C gravimetrically (Martin-Polo, Voilley, Blond, Colas, Mesnier, & Floquet, 1992), using a saturated $Mg(NO_3)_2$ solution as the internal relative humidity environment (RH ≈ 53%) of glass cells (cylindrical configuration allowing an effective film diameter of 4.3 cm) which were placed in an external environment of 100% RH; the air gap between the film and the surface of the saturated salt solution was kept constant at 1.0 cm. Film thickness was measured at five locations on each specimen with a hand-held micrometer, and the mean value was used for WVP calculation.

3. Results and discussion

3.1. Water sorption

Isotherms of pullulan/starch, ps, blends or of the two polymers separately were sigmoid in shape (Fig. 1), typical of high molecular weight hydrophilic polymers and of most foods with high starch or protein content. Among all the blends, the free-polyol specimen (ps) had the highest equilibrium water content at low and medium water activities than samples plasticised with sorbitol (ps/s) or xylose (ps/x). This was not a surprise considering that monosaccharides or products of high sugar content usually exhibit a long flat segment in their sorption isotherm within the a_w range of 0.1–0.6, and rapid increases in their water content at water activities above 0.6–0.8. The latter was also evident in the ps/s and ps/x blends at a_w above 0.75 where the moisture content of the polyol-plasticised blends by far exceeded the respective values of the ps blend. These changes in water sorption affinity at low vs. high a_w environments are even more pronounced when higher amounts of polyols were included in the blends (data not shown). A direct consequence of such variation in the hydration properties of different constituents would be the unequal partitioning of water among them in a composite sample; e.g. at low a_w, the polysaccharides would have higher water content than the polyols, whereas the reverse is expected at high a_w. This preferential partitioning of water may in turn have a substantial effect on plasticisation of the polysaccharides, particularly in the low moisture content range, thus complicating the theoretical modelling for prediction of T_g of biopolymer–sugar blends from the respective behaviour of separate components (Kalichevsky et al., 1992b, 1993b; Kalichevsky & Blanshard, 1993). It has been widely claimed in the literature that the shape of the isotherm of a multicomponent system can be calculated from the weighted average of the sorption data of the individual components when the following conditions are met (Rahman, 1995): (a) equal water activity by all components in the mixture at equilibrium; (b) if water is transferred between components during equilibration, at any given a_w, each component will reach a moisture content equal to that obtained from its individual sorption isotherm. In reality, however, it has been demonstrated how difficult is to determine the water partitioning and apply the additivity principle, in respect to the mass fractions of the components, for biopolymer mixtures (Hartley, Chevance, Hill, Mitchell, & Blanshard, 1995; Kaminski, & Al-Bezweni, 1994). For binary starch-containing systems (starch–egg white and starch–xanthan gum), less water was found to be associated with the starch component than would be expected if considering starch alone in the a_w range of 0.2–0.9 (Hartley et al., 1995); accordingly, an interaction parameter, ξ', was introduced to rectify this abnormality. Although the exact

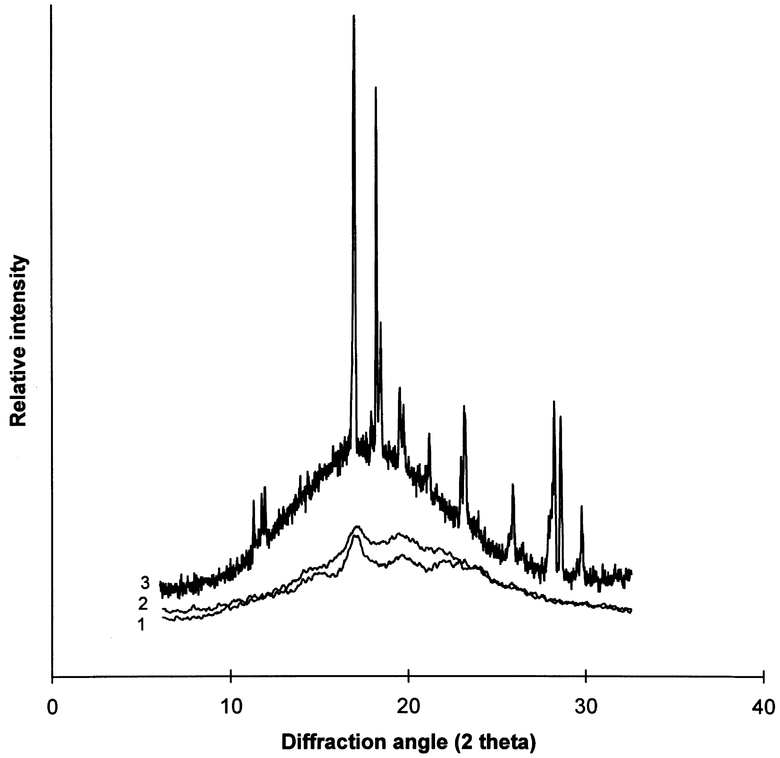

Fig. 2. X-ray diffractograms of ps/x20 blend after storage for two weeks at RH 94% (1) or RH 64% (2), and of an admixture of pullulan/gelatinised corn starch and crystalline xylose (3) in the same weight ratio as in the blend.

nature of this non-ideal behaviour is obscure, it points to the non-equilibrium state of multicomponent systems as repeatedly advocated by Slade and Levine (1991, 1993).

The values of the fitting parameters for the BET and GAB adsorption models are sammarised in Table 1, whereas representative plots for the ps blend are shown in the inset of Fig. 1. The range of monolayer moisture values was similar between the two models (6.0–9.2 for BET and 6.0–9.9 g H_2O/100 g for GAB). The GAB isotherm successfully described the water sorption data up to the a_w of 0.9, confirming the applicability of this equation to sorption data in the multilayer region (van den Berg & Bruin, 1981). The three-parameter GAB model has been proven reliable in modelling sorption data for many food materials (Bizot, 1983; Rahman, 1995), including polysaccharides (Weisser & Liebenspacher, 1989; Bizot et al., 1997). In contrast, the BET model was applicable only within the a_w range 0–0.64 for all composite systems examined (Table 1). The sorption affinity of the ps blend was largely governed by the hydration properties of the pullulan, primarily in the upper a_w range. Bizot et al. (1997) have also demonstrated higher water uptakes for pullulan, dextran and amylodextrins compared to native starch at a_w above 0.7. At high water activities, incorporation of sorbitol or xylose (as co-plasticisers) at 10 and 20% w/w d.b. greatly increased swelling and the equilibrium moisture content of the composite films; specimens with 10 (ps/s10 and ps/x10) or 20% d.b. polyol (ps/s20 and ps/x20) were converted into swollen gels at a_w above 0.84. In this region of the isotherm, however, the accuracy of moisture determination falls quickly as water content values are largely affected by osmotic and capillary phenomena because of changes in the structure (and accessible surface) of the material.

Phase changes (e.g. crystallisation) are also known to affect the sorption isotherms as crystalline materials normally display limited sorption. For example, crystallisation of sugars on humidification of food products (e.g. lactose in dry milk powders) leads to moisture release and a concomitant break in the sorption isotherm (i.e. equilibrium water content decreases). As crystallisation is time- and material composition-dependent as well as it decreases with decreasing a_w, the amount of water sorbed is incorrectly predicted by modelling the sorption data (Jouppila & Roos, 1994). Owing to the incorporation of gelatinised corn starch and monomeric polyols in the composite films, after equilibration all samples were examined by X-ray diffraction for crystallinity development. Only for films stored at a_w above 0.64 there was evidence for partial crystallisation of the starch component from the development of the characteristic d-spacing at 15.8 Å of the B-pattern of retrograded starch (Biliaderis, 1998), as shown in Fig. 2. Soest et al. (1996a) have observed rapid increase in B-type crystallinity and changes in the mechanical properties of thermoplastic potato starch within two weeks storage at 70 and 90% RH. Rindlav, Hulleman, and Gatenholm (1997) also reported increasing crystallinity (B-type) in potato

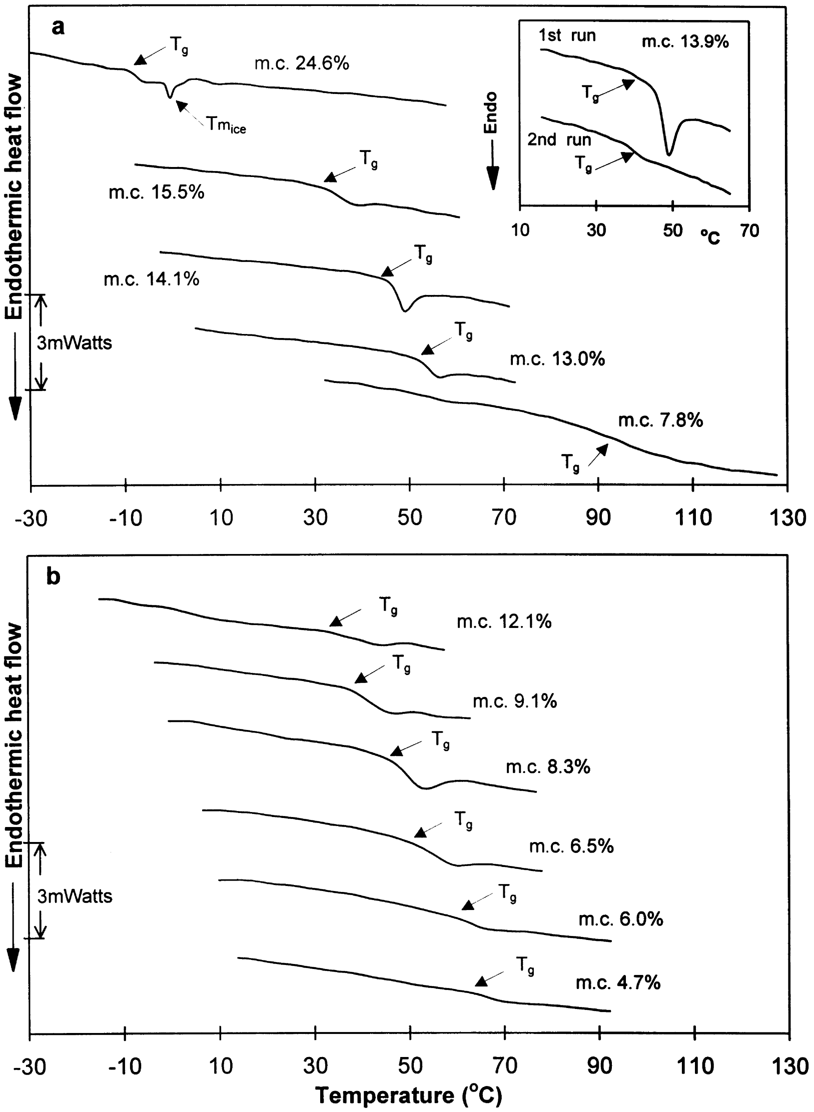

Fig. 3. DSC scans for ps (a) and ps/s10 (b) blends at different water contents; arrows indicate the position of the middle temperature for the glass transition obtained from the rescan traces.

starch films stored at above 58% RH. As for the sorbitol or xylose, there was no indication of any crystallisation of these sugars in the films or thicker specimens at all relative humidity environments (Fig. 2). Thus, crystallisation of the sugars seems to be hindered when they are dispersed in the composite pullulan–starch matrix, presumably attributable to decreased solute diffusivities.

3.2. Thermal transitions

The effect of water on the DSC thermal traces of two representative samples (ps and ps/s10) is demonstrated in Fig. 3. The initial scans of most specimens showed endothermic transitions for the polymeric components of the blend. The temperature location and magnitude of this transition was dependent on sample composition (water and polyol contents). Such endothermic events have been previously reported at sub-T_g temperatures for starch and other polysaccharides at low moisture levels (Appelqvist et al., 1993; Bizot et al., 1997; Forssell et al., 1997; Kalichevsky et al., 1992a; Livings et al., 1997; Shogren, 1992; Yuan & Thompson, 1994). Specific interactions (enthalpic associations) between water and hydroxyl groups of the amorphous polysaccharides were first suggested as contributing to the sub-T_g endotherm by Gidley and co-workers (Appelqvist et al., 1993; Gidley, Cooke, & Ward-Smith, 1993). However, the current consensus for the structural origin of this endotherm favours an enthalpy relaxation mechanism (Livings et al., 1997; Shogren, 1992; Thiewes & Steeneken, 1997), a common feature of physical aging of many synthetic polymers and their blends (Berens & Hodge, 1982; Hodge & Berens, 1982). Glasses are generally regarded as solidified supercooled liquids whose volume, enthalpy and entropy are greater than they would be at

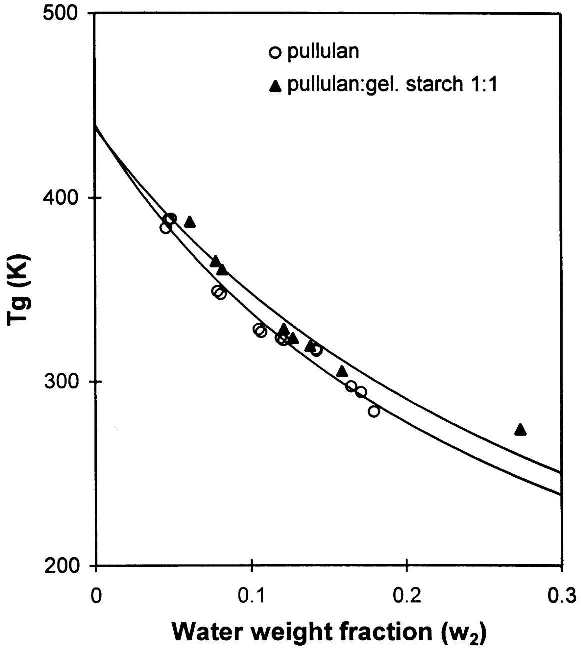

Fig. 4. Relationship of glass transition and moisture content for pullulan and pullulan/gelatinised corn starch; the solid lines give the G–T plots of the experimental data (best fit).

equilibrium. Such non-equilibrium structures would relax, through local motions, towards a lower energy state (enthalpy and volume relaxations) on aging at sub-T_g temperatures (between T_g and T_β); e.g. a very 'open' glass structure produced by rapid thermal quenching densifies through volume reduction on annealing (there is a decrease in entropy of the solid). Consequently, physical aging of glasses at sub-T_g temperatures affects several material properties including density, creep, stress-relaxation, dielectric constant and dielectric loss, and it clearly demonstrates that molecular mobility could exist below the glass transition temperature. The development of sub-T_g heat capacity peaks (enthalpy relaxation or enthalpy recovery) has been shown to increase with increasing annealing time and temperature, relative to T_g (Berens & Hodge, 1982). The evolution of the DSC endothermic peak provides a quantitative means to follow enthalpy relaxation kinetics of amorphous materials on aging. For the ps blends, endothermic peaks in the DSC traces were more pronounced at intermediate water contents; i.e. the enthalpy relaxation will manifest itself if there is sufficient mobility for the chains to move towards the equilibrium. Thus, the more dry (or polyol deficient) ps blends, having relatively high glass transition temperatures, underwent negligible aging during storage at room temperature due to large $\Delta T = T_g - T_{storage}$. In contrast, for the highly plasticised samples (i.e. T_g is close to the storage temperature) certain amorphous domains in the ps blends would undergo sufficient plasticisation, yielding a somewhat weaker and broader transition in the T_g region. Livings et al. (1997) have recently studied the effects of aging on wheat flour-based confectionary wafers. It appeared from DSC, X-ray and IR data that the starch polymers undergo molecular rearrangements during the relaxation process; i.e. formation of single helical (V_h) chains. It must be noted, however, that aged pullulan (only) specimens, conditioned at various moisture levels, also exhibited pronounced enthalpy relaxation endotherms and that there is no evidence for molecular ordering of this polymer considering the great chain flexibility around the α-(1 → 6) glycosidic linkage (three rotational degrees of freedom, instead of two for α-(1 → 4) linkages).

The measurement of the glass transition temperature of a polymer mixture is often used as a criterion to establish its miscibility. A miscible polymer mixture would exhibit a single transition between T_gs of the two components. With increasing immiscibility there is a broadening of the transition, whereas an incompatible system would be marked by separate transitions of the polymer components in the blend. For all the water- and/or polyol-plasticised ps blends, a single glass transition was observed in the DSC traces for the polymer components. This behaviour does not necessarily imply miscibility between pullulan and starch at a molecular or segmental level, in view of the well-reported incompatibility between α-D-glucans (amylose, amylopectin, dextran) in dilute solutions (Kalichevsky, Orford, & Ring, 1986; Kalichevsky & Ring, 1987). It could merely reflect the manifestation of two closely occurring (but independent) α-relaxation processes of the two polymeric components. According to Olabisi, Robeson, and Shaw (1979), it is not possible to differentiate a phase separated system from a miscible one by calorimetry if the component T_gs are less than 20°C apart. Thus, Kalichevsky and Blanshard (1992) were able to show by DSC and DMTA dual glass transitions for water-plasticised gluten–amylopectin and gluten–casein blends, and a single transition for the casein–amylopectin system. Although all mixtures of these biopolymers appear to be immiscible, small differences in T_ss between casein and amylopectin (∽ 10°C at most water contents of the blend) did not allow the manifestation of dual transitions. In contrast, substantial differences in chemical structure and hydrophobicity of gluten compared to amylopectin (or casein), reflected by a large divergence in T_gs (∽ 20–50°C), makes it possible to detect individual transitions of the two polymers by DSC. A single α–relaxation was also reported for white bread (a composite matrix of starch and gluten) by mechanical spectroscopy (Roudaut, 1998), clearly indicating the difficulty of separating glass transition events of individual constituents in composite products. Bizot et al. (1997) have recently measured the T_gs of a wide range of polysaccharides differing in their molecular weight, degree of branching and glycosidic linkages. For the high molecular weight glucans, the reported differences in T_gs were between 5 and 30°C in the water content range of 5–25%. Moreover, all polysaccharides exhibited almost parallel trends in their T_g-moisture content plots, indicative of similar plasticisation responses. It can be concluded from this that the close

Table 2
Estimated glass transition temperatures of pullulan and pullulan/corn starch blends using the Gordon–Taylor equation with varying values for the *k* parameter

Sample	Best fit			$k = 4.13$		$k = 3.89$	
	T_{g_1}	k	r^2	T_{g_1}	r^2	T_{g_1}	r^2
p	439.9	4.55	0.99	431.1	0.99	425.9	0.99
ps	438.3	3.81	0.99	446.5	0.99	440.2	0.99
ps/s10	358.3	2.51	0.99	383.6	0.98	380.0	0.98
ps/s20	332.2	1.93	0.99	363.3	0.93	360.3	0.94
ps/x10	379.3	3.57	0.99	388.3	0.99	384.5	0.99
ps/x20	367.2	4.06	0.99	368.2	0.99	364.8	0.99

proximity in T_gs between starch and pullulan does not allow for a clear calorimetric distinction of the glass transitions of these polymers in the ps blends.

Modelling of T_g depression by water for all specimens, using the empirical G–T equation, has proven useful in fitting the experimental T_g data and moisture content. It should be noted, however, that application of this equation as well as that of Couchman and Karasz (1978) assumes component miscibility at a segmental level, a condition that is unlikely to be met with the water- and polyol-plasticised ps blends. Moreover, with the existing limitations in sample preparation and the DSC methodology (limiting cooling rates) it is not feasible to obtain data for water weight fractions in the blends above 0.4. Despite the theoretical limitations, the G–T equation can be applied in a purely empirical sense to describe the water content dependence of T_g of biopolymers and their mixtures. As glass transition temperature was assigned the middle temperature of the transition from the second DSC scan to eliminate the enthalpy relaxation peaks and standardise the cooling history of the sample; for most samples this temperature was found to coincide with the onset of the transition of the first thermal scan. Fig. 4 shows the composition dependence of T_g of pullulan and ps blend, while the parameters of all G–T plots (T_g of dry polymer blend and *k* constant) are sammarised in Table 2. Further to the best fit (where optimisation is sought for both parameters) two additional curve fittings were considered by allowing *k* to take a constant value. As the constant *k* of the G–T equation is equivalent to the ratio of heat capacity changes at T_g of the pure diluent (water) and the polymer matrix, $\Delta Cp_2/\Delta Cp_1$, two estimates of this ratio can be calculated from literature data. A heat capacity change increment at T_g for starch of $\backsim 0.47\ \mathrm{J\,g^{-1}\,K^{-1}}$ was reported by Orford, Parker, Ring, and Smith (1989), whereas two ΔCp values for water may be assumed: $1.94\ \mathrm{J\,g^{-1}\,K^{-1}}$ (Sugisaki et al., 1968) and $1.83\ \mathrm{J\,g^{-1}\,K^{-1}}$ (Hatley & Mant, 1993). Therefore, the $\Delta Cp_2/\Delta Cp_1$ ratio of 4.13 or 3.89 may be considered as a reasonable value for *k*. With either one of the two values of *k*, the fits were reasonably good ($r^2 > 0.93$), giving T_g estimates for the dry ps in the range of 440–446 K, much higher than the pullulan only. This T_g elevation can be also inferred from the lower T_g values reported for pullulan (~10–25°C) compared to the starch polymers at similar hydration levels (Bizot et al., 1997). For the polyol-plasticised blends, there was a substantial reduction in the T_g with increasing polyol level in the blend. Also, at equivalent polyol concentration, sorbitol seemed to depress the T_g more of the ps blend than xylose (Table 2).

The mechanical behaviour of the blends at the glass transition zone was also examined by dynamic mechanical thermal analysis. For all samples, the one-step drop in elastic modulus (E') at T_g ($\backsim 10^{2.0}$–$10^{2.5}$ Pa) as well as the single peak in tan δ (Fig. 5) were consistent with the DSC results; i.e. there was no indication for separate transitions of the two polymeric components in the blends. With increasing water content an increased breadth (tan δ) of the transition

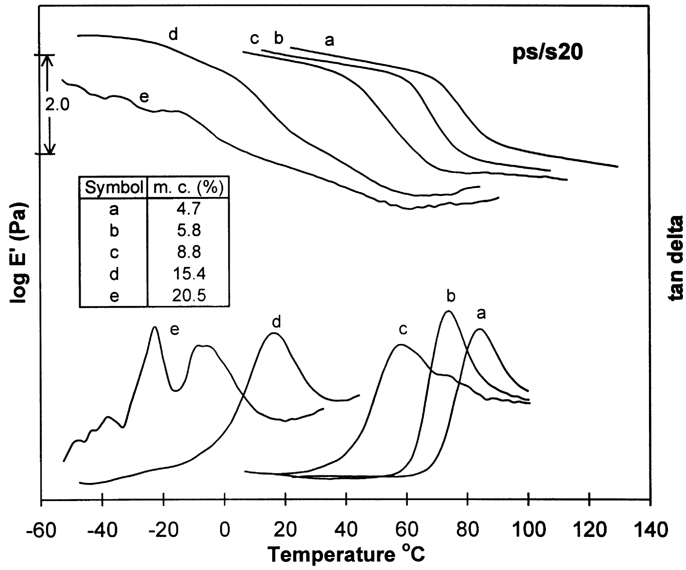

Fig. 5. DMTA log E' and tan δ for ps/s20 at different moisture contents.

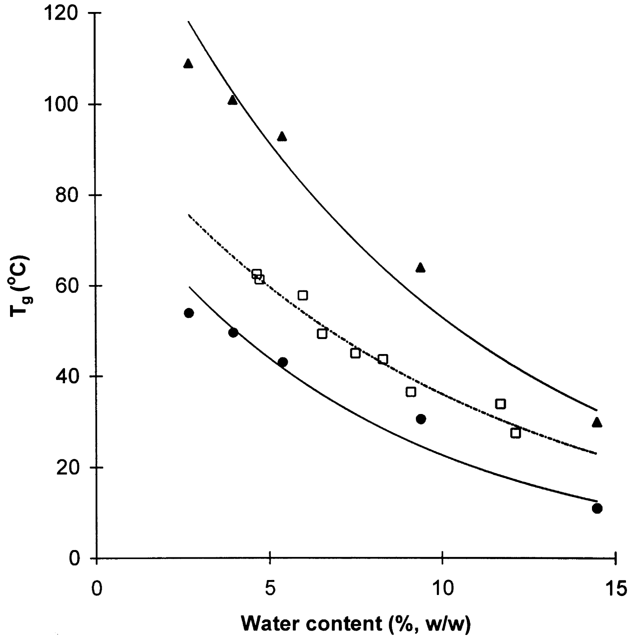

Fig. 6. T_g of ps/s10 as defined from the peak tan δ (top), DSC (middle) and onset of elastic modulus (E') drop (bottom); DSC at 5°C min^{-1} and DMTA at 2°C min^{-1} (1 Hz).

was observed, implying a broader distribution of relaxation times. However, there was no evidence for a polyol-rich phase (which may be owing to phase separation of polyol and the polymer mixture), presumably because of low levels of polyols (10 and 20% d.b.) employed in the blends. The low temperature transitions seen with some highly plasticised ps blends (e.g. ps/s20, 20.5% moisture, Fig. 5(e)) are most likely artifacts due to ice melting and the difficulty to properly tighten such high moisture content specimens in the DMTA analyser. The DMTA results of fructose-plasticised amylopectin by Kalichevsky and Blanshard (1993) also did not reveal a separate transition for the polyol component in the blend up to a 20% d.b. level. It was only at high sugar contents, i.e. a sugar/polymer (amylopectin, gluten, caseinate) ratio of 1:2, where two transitions (from the polymer-rich and polyol-rich phases) were observed, suggesting the occurence of phase separation (Kalichevsky & Blanshard, 1993; Kalichevsky et al., 1993a, 1992b). The relative order of the characteristic temperatures of the glass–rubber transition of the ps blends, as probed by DSC and DMTA, is shown in Fig. 6 for the ps/s10 sample. In general, the DSC transition temperatures fell in between the onset of E' drop and the peak tan δ (at 1 Hz), in agreement with the findings of Kalichevsky et al. (1992a) on amylopectin and of Kalichevsky and Blanshard (1993) on amylopectin/fructose mixed systems. These results further point to the difficulty of assigning a single temperature for the glass–rubber transition of hydrated biopolymer mixtures. Even for single components (e.g. starch) the glass transition entails changes over a temperature range of 10–20°C (Biliaderis, 1998; Vodovotz & Chinachoti, 1996) and, therefore, it would be more appropriate to characterise and report the T_g as a temperature range of transitions.

The dynamic mechanical tan δ peaks shift to higher temperatures with increasing measurement frequency (Fig. 7(a)). The sensitivity of α-relaxation processes to frequency permits its discrimination from structural changes such as crystallisation or melting. The apparent activation energy (ΔH_a) for the α-relaxation can be thus determined from the Arrhenius rate relationship

$$\ln f = -(\Delta H_a/RT).$$

Fig. 7(b) shows the variation of T_g (peak tan δ) as a function of the frequency of mechanical oscillation (1–20 Hz) for

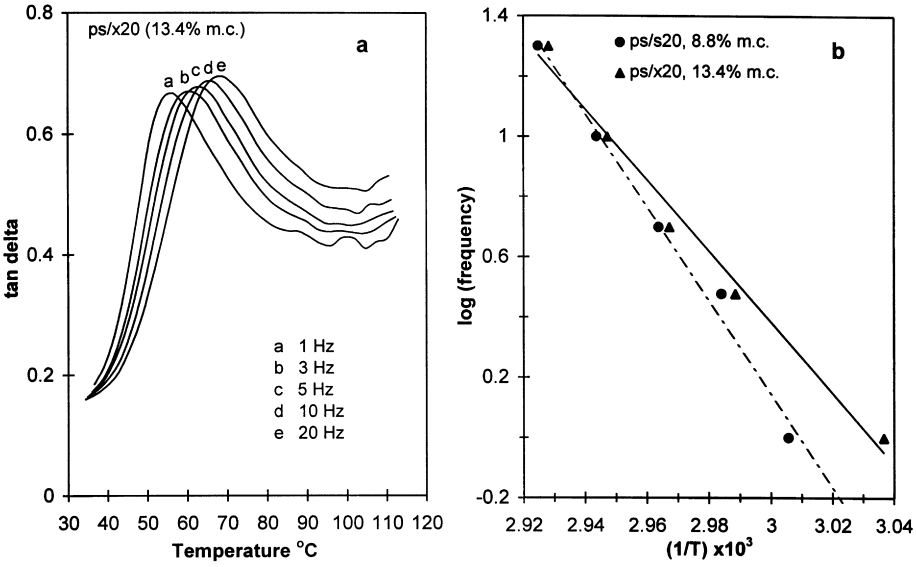

Fig. 7. Multifrequency DMTA tan δ of thermal scans for ps/x20 (a) and plots of log$f$ against reciprocal temperature for ps/s20 and ps/x20 to determine the activation energy of the α-relaxation process (b).

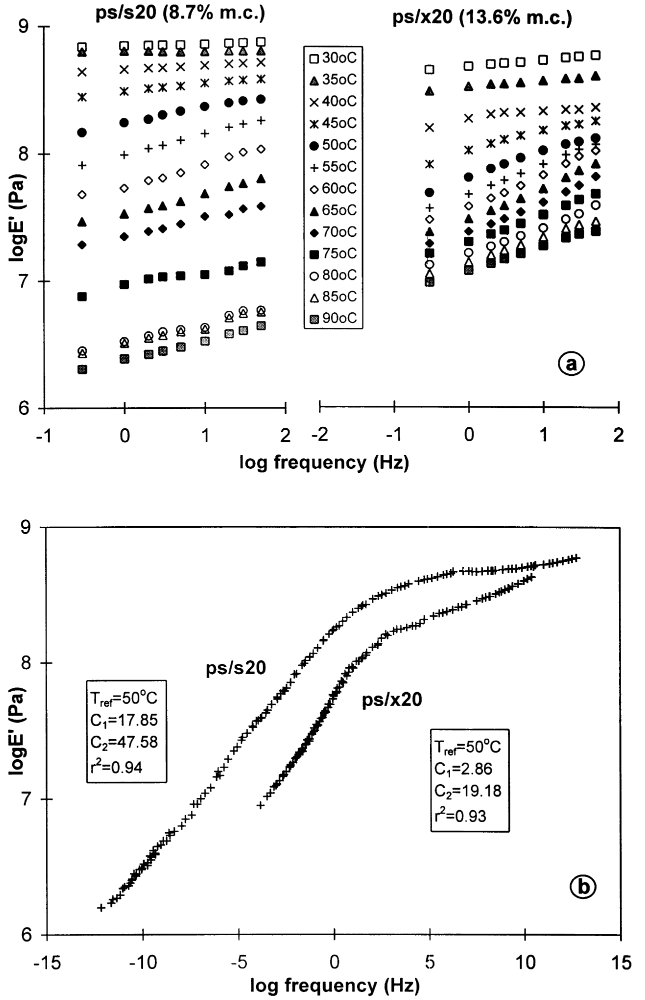

Fig. 8. Modulus-frequency curves (a) and master curves of log E' against frequency for ps/s20 and ps/x20.

two blends. The calculated activation energies ps/s20 (8.8% moisture) and ps/x20 (13.4% moisture) were 296 and 226 kJ mol^{-1} for the ps/s20 and ps/x20, respectively. These values are close to those reported for synthetic polymers in the absence of plastisiser (351 kJ mol^{-1}) (Sperling, 1986) and amorphous wood components ($\sim$ 340 kJ mol^{-1} at 15% m.c.) (Kelley, Rials, & Glasser, 1987). Over similar frequency ranges, for white bread samples with 0 and 5% moisture, values of 424 and 370 kJ mol^{-1}, respectively, were reported (Le Meste et al., 1996), whereas a gluten sample with 12.9% moisture gave an apparent activation energy of 242 kJ mol^{-1} (Kalichevsky et al., 1992b). Moreover, MacInnes (1993) has found activation energies of 200–300 kJ mol^{-1} for glass transitions in 80% sucrose solutions. These high activation energy values for α-relaxation processes, compared to β- and γ-transitions, are indicative of large degree changes in segmental mobility and a high degree of co-operativity.

From the apparent activation energies, a ‘fragility’ parameter, m, can be calculated using the following relationship:

$$m = (-\Delta H_a/2.303RT_g).$$

This parameter, introduced by Angell to simplify the applicability of the concept of ‘strong/fragile’ glass-forming liquids, is the slope of the T_g-scaled Arrhenius plot of any relaxation time (or any property, such as viscosity, which is proportional to a relaxation time) measured at T_g (Angell, Bressel, Green, Kanno, Oguni, & Sare, 1994). Thus, ‘strong’ materials are those for which the temperature coefficient for a mechanical property does not vary much with increasing temperature above T_g. In contrast, ‘fragile’ materials show a strong decline in their mechanical properties above T_g. Using the given equation, the derived ΔH_a values from the DMTA data and the glass transition temperatures estimated from the G–T plots, the parameter m was calculated for the two blends: $m = 51$ for ps/s20 (at 8.8% m.c.) and $m = 42$ for ps/x20 (at 13.4% m.c.). These values are in close agreement with estimates of m for other biopolymers at low hydration levels: $m = 40.5 \pm 2.0$ for poly-L-asparagine (15–24% m.c.) (Angell et al., 1994); $m = 43$ for elastin ($\sim$ 22% m.c.) (Lillie & Gosline, 1993); $m = 40$ for gluten ($\sim$ 13% m.c.) (Kalichevsky et al., 1992b). Such values of m are indicative of relatively ‘strong’ materials according to Angell’s classification; i.e. these materials are structurally resistant when heated above their T_gs. The practical implications of the ‘strong’/’fragile’ behaviour of food constituents with respect to stability of glassy food products have been recently discussed by Simatos, Blond, and Perez (1995). From the definition of fragility and its characterising parameter m (slope at T_g of the scaled Arrhenius plots), we may expect that small variation in the value of m among materials would result in large differences in their stability on storage for an ‘equivalent’ raise in temperature (T/T_g).

It has been often demonstrated that viscoelastic data collected at one temperature (and multiple frequencies) can be superimposed upon data collected at a different temperature simply by shifting one of the curves along the time (or frequency) axis (Williams, Landel, & Ferry, 1955; Ferry, 1980); i.e. there is equivalency between time (frequency) and temperature as they affect material properties of polymers. The time–temperature superposition (TTS) principle is based on the premise that processes involved in molecular relaxations occur most rapidly at high temperatures. Thus, viscoelastic changes which occur relatively quickly at higher temperatures can be made to appear if they have occurred at lower temperatures simply by shifting the data with respect to time. In this respect, viscoelastic data can be collected by performing measurements at multiple frequencies under isothermal conditions and repeating such measurements at several temperature steps (Fig. 8(a)). By selecting a reference temperature, shifting the other data with respect to time and superimposing them upon the selected reference curve, a master curve can be obtained. An important benefit of generating a master curve (Fig. 8(b)) is the ability to extend the measurements in mechanical properties over a much broader frequency range, often inaccessible by practical experiments. The degree of horizontal (time) shifting required to superimpose

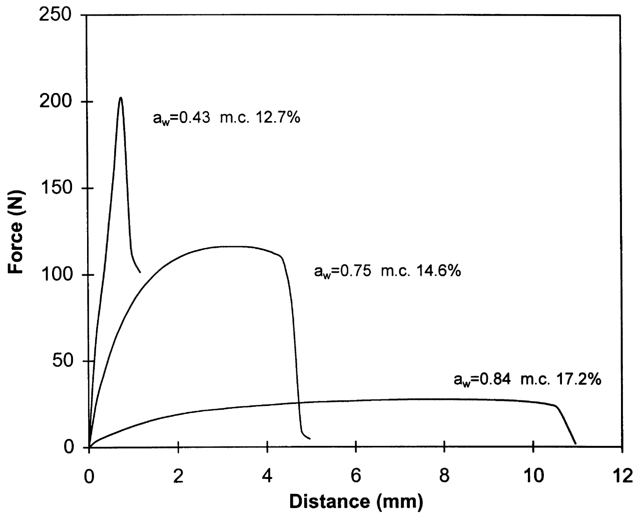

Fig. 9. Load-deformation curves (tensile) for ps/s10 at different moisture contents.

a given set of data with respect to a reference curve can be described by the Williams–Landel–Ferry (WLF) equation

$$\log\alpha_T = -C_1(T - T_0)/C_2 + T - T_0,$$

where α_T is the shift factor, C_1 and C_2 are constants (for many amorphous polymers they generally assume the ‘universal’ values of 17.4 and 51.6, respectively), and T_0 is a reference temperature (e.g. T_g). Using the superposition (WLF) software of the DMTA analyser, master curves of the log E' (dynamic elastic modulus) were generated for the ps/s20 and ps/x20 blends (Fig. 8(b)). For the ps/s20 blend, the derived best fit values for C_1 (17.8) and C_2 (47.6) were in close agreement with the ‘universal’ constants. In contrast, the corresponding C_1 and C_2 values for the ps/x20 largely differ from the ‘universal’ values of the WLF constants. The TTS analysis was also applied to solvent-plasticised amylose (Nakamura & Tobolsky, 1967) and wood (Kelley et al., 1987) where the applicability of the WLF equation was shown over a limited range of temperatures.

3.3. Mechanical properties and physical state

Some typical force–distance diagrams of ps/s10 blends at three moisture contents are shown in Fig. 9, whereas the results from the tensile tests of the ps/s and ps/x are given in Table 3. At moisture contents less than 7–9%, the specimens were glassy at room temperature exhibiting very high Young’s moduli and limited elastic deformation before rupture, typical of brittle behaviour. With increasing plastisiser (water, polyol) content there was a gradual change from brittle to ductile failure, the latter being characteristic of a polymer plasticised through its glass transition temperature. This state transition is accompanied by sharp decrease in modulus and tensile strength, and an increase in elongation (Table 3). Similar observations of moisture effects on tensile modulus and tensile stress have been made for starch films and starch-based composite materials (Arvanitoyannis & Biliaderis, 1998; Bader & Goritz, 1994; Fontanet, Davidou, Dacremont, & Le Meste, 1997; Lawton, 1996; Soest, Wit, & Vliegenthart, 1996b). The ps/polyol blends exhibited maximum elongation at intermediate moisture levels (15–20%), confirming the findings of Soest et al. (1996b) on thermoplastic waxy corn starch. For the ps blends, with increasing polyol level (from 10 to 20% d.b) there was a pronounced decrease in modulus and tensile strength, whereas the percentage elongation showed a substantial

Table 3
Tensile modulus, tensile strength and percentage elongation of polyol- and water-plasticised pullulan/ corn starch blends

Gelatinised starch	Pullulan	Sorbitol	Water	Tensile modulus (MPa)	Tensile strength (MPa)	Elongation (%)
45	45	10	7.6	774.0 ± 59.3	16.8 ± 4.2	2.5 ± 0.7
45	45	10	9.1	720.7 ± 139.2	19.3 ± 6.1	2.8 ± 0.5
45	45	10	11.8	105.6 ± 21.2	4.3 ± 0.9	18.4 ± 4.3
45	45	10	15.6	19.0 ± 4.3	1.4 ± 0.2	35.2 ± 7.7
45	45	10	21.4	1.1 ± 0.3	0.1 ± 0.02	15.6 ± 3.5
40	40	20	8.5	655.5 ± 48.4	21.9 ± 2.4	3.9 ± 0.6
40	40	20	10.0	457.9 ± 35.2	13.2 ± 2.3	5.1 ± 1.4
40	40	20	12.2	93.1 ± 19.1	3.9 ± 0.7	25.9 ± 5.2
40	40	20	15.8	9.1 ± 1.5	1.1 ± 0.1	61.9 ± 11.9
40	40	20	18.9	5.4 ± 0.9	0.4 ± 0.07	21.6 ± 3.9
		Xylose				
45	45	10	9.9	1978.5 ± 192.5	22.7 ± 5.4	2.6 ± 0.4
45	45	10	11.9	1007.1 ± 157.8	27.6 ± 7.6	2.8 ± 0.5
45	45	10	14.9	496.1 ± 106.5	15.8 ± 2.9	3.9 ± 0.6
45	45	10	20.9	17.4 ± 3.4	1.1 ± 0.2	43.7 ± 11.8
45	45	10	33.9	0.4 ± 0.1	0.04 ± 0.01	21.7 ± 4.2
40	40	20	13.2	670.4 ± 43.1	14.6 ± 2.1	2.3 ± 0.3
40	40	20	13.7	572.8 ± 52.9	12.9 ± 2.6	2.4 ± 0.2
40	40	20	14.6	203.6 ± 32.6	5.9 ± 0.9	9.8 ± 2.1
40	40	20	17.2	27.6 ± 6.1	3.0 ± 0.7	58.1 ± 12.5
40	40	20	25.0	3.8 ± 0.9	0.2 ± 0.04	18.3 ± 4.1

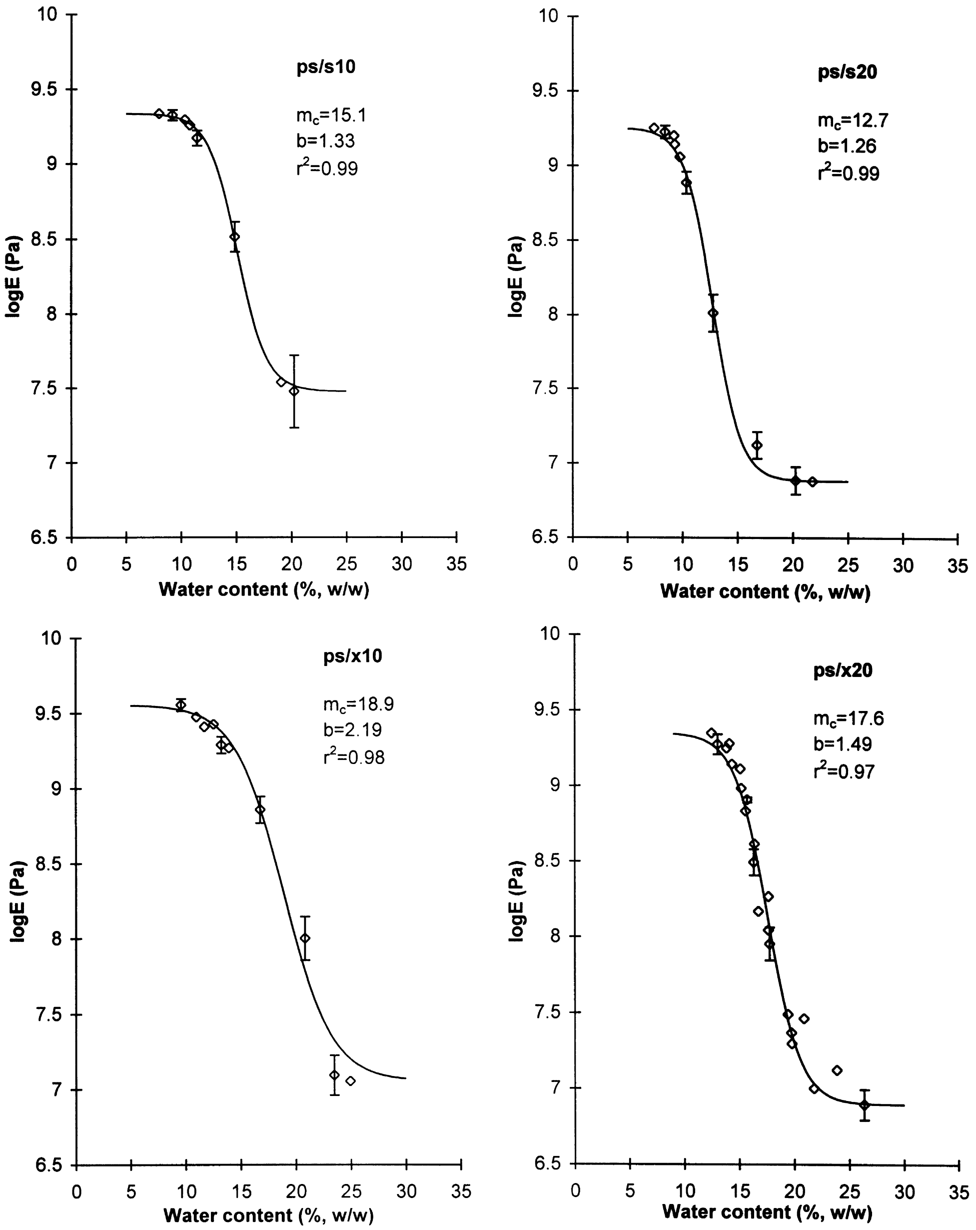

Fig. 10. Flexural modulus against water content of different pullulan/gelatinised corn starch/polyol blends; the solid lines represent the fit of the data with Fermi's model.

increase. The effect of low molecular weight polyols on the mechanical properties of ps blends is related to their plastisising properties (i.e. they depress the T_g of the polymer mixture), as has been shown for pure starch and other biopolymers (Arvanitoyannis, Kalichevsky, Blanshard, & Psomiadou, 1994; Cherian et al., 1995; Gontard, Guilbert, & Cuq, 1993; Kirby, Clark, Parker, & Smith, 1993; Ollett, Parker, & Smith, 1991). The depression of T_g in water- and polyol-plasticised systems may be attributed to the additional free-volume provided by the plastisiser, which allows high segmental mobility at lower temperatures. It was of interest also to note that at equivalent polyol level, sorbitol, despite its higher molecular weight, exhibited a stronger plasticising action than xylose (lower modulus and tensile strength). Further to the amount and type of polyol, several other factors are known to affect the tensile properties of biomaterials containing starch such as method of specimen preparation (extent of destructurisation, orientation effects and macrostructure), amylose content, formation of amylose–lipid complexes and crystallinity (physical cross-linking) due to aging at high relative humidities (Bader & Goritz, 1994; Lawton, 1996; Lourdin, Della Valle, & Colonna, 1995; Shogren, 1992; Soest et al., 1996a,b).

Fig. 10 illustrates the effect of water content on flexural modulus, determined by the three-point bend test, of the ps/polyol blends. At low moisture levels ($<$ 10%) the moduli were relatively high. With increasing moisture content each blend exhibited a sharp drop in modulus (~ 2.5–3.0 orders

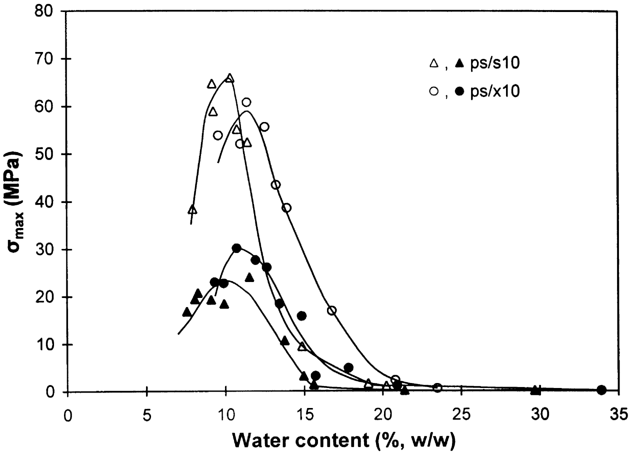

Fig. 11. Relationship of water content and maximum stress (σ_{max}) from flexural (open symbols) and tensile (closed symbols) tests of the ps/s10 and ps/x10 specimens.

of magnitude). The fall in *E*, reflecting the glass–rubber transition, occurs at a water content which is dependent on the polyol level in the blend, and is typical of the influence of plastisisers on synthetic polymers (Platzer, 1965). The sigmoid relationships of Fig. 10 have been previously shown for amylopectin and starch containing materials (Arvanitoyannis et al., 1996; Arvanitoyannis & Biliaderis, 1998; Kalichevsky et al., 1992a; Kalichevsky & Blanshard, 1993; Kirby et al., 1993; Ollett et al., 1991). Between the two polyols, the glassy plateau moduli of the ps/x samples were slightly higher than those of ps/s, which is consistent with the data from tensile testing (Table 3). Modelling of the data with Fermi's equation enables the comparison among samples for the fall in modulus (around the glass transition) as a function of moisture content under isothermal conditions (Peleg, 1996a,b). The regression parameters (m_c and *b*) of the Fermi's distribution function for each sample are included in Fig. 10. For each ps/polyol system, the m_c value decreased (i.e. the fall in *E* occurred at a lower moisture content) and the transitions became sharper (lower value of *b*) with increasing level of polyol. Moreover, the fall in modulus was steeper and centered at a lower m_c for the ps/s samples compared to their ps/x counterparts. The observed changes in modulus as a function of water content (Fig. 10) clearly illustrates a succession of processes in material structure and properties, adding further support to the notion that the glass transition is not an abrupt event, particularly in complex food systems (Harris & Peleg, 1996). According to the studies of Nicholls et al. (1995) on fracture behaviour of gluten and starches in the glassy state, the glass transition has a different effect on material properties for different biopolymers. Specifically, brittleness (crunchy or crispy textures) could not be predicted on the basis of known T_g alone, because biopolymers may exhibit different fracture mechanisms in the glassy state.

A thorough examination of the relationship between maximum stress (from both tensile and flexural testing) and moisture content showed similar bell-shape responses for the ps/s10 and ps/x10 blends (Fig. 11). The most salient feature of these plots is the apparent increase in stiffness as the moisture content arises from 7 to 11%, whereas the softening effect of water becomes dominant above this level. Data showing similar trends in stiffening of glassy biopolymers at low moisture levels have been previously reported (Attenburrow, Davies, Goodband, & Ingman, 1992; Fontanet et al., 1997; Harris & Peleg, 1996; Nicholls et al., 1995). A similar relationship was also presented for the Young's modulus, derived from compression tests, of extruded flat bread by Fontanet et al. (1997), a finding that was not confirmed by the results of the present study (Fig. 10). Several suggestions have been made to explain such material toughening on partial plasticisation with water. According to Harris and Peleg (1996), glassy biopolymers at low moisture are extremely brittle and very fragile, offering no resistance to applied load. With low levels of hydration, the plasticised matrix becomes more cohesive, more structural elements remain intact (offering more resistance to fracture), and the material would deform rather than disintegrate on compression. Fontanet et al. (1997) have ascribed the hardening phenomenon to short range reorganisation of the material as a result of increased molecular mobility by adding small amounts of water; partial plasticisation with water would foster aging phenomena in the glass, leading to a denser structure. These authors have also offered an alternative hypothesis, attributing material toughening to formation of micro-shear bands (caused by slight increase in free-volume) during compression testing. Further work is required to enhance the knowledge of the molecular mechanisms controlling the mechanical and other material properties of biopolymers at low hydration.

3.4. Gas and water vapour permeability

GP and WVP of polymeric materials are important attributes when one considers barrier properties of films and coatings. Despite the wide availability of synthetic polymers and polymer laminates that are excellent barriers to gasses and aroma, environmental and economic reasons have stimulated interest in developing edible films and coatings based on polysaccharides and/or proteins. Hydrocolloid films, because of their hydrophilic nature have poor resistance to water vapour transfer, but are good barriers to oxygen, carbon dioxide, and lipids. Although permeability is simply defined by the product of solubility and diffusivity, the relationships between barrier characteristics and polymer structure are fairly complex. Several polymer properties influence mass transport phenomena in films: chemical structure and molecular weight, polymer processing conditions, free-volume effects (chain packing), crystallinity, polarity, orientation, cross-linking, presence of additives, addition of fillers and polymer blending. For example, desirable characteristics for a good oxygen barrier include: high-chain stiffness, some intermolecular cross-linking and

Table 4
GP (O_2 and CO_2) at 22°C and glass transition temperatures (T_g) determined from the inflection of GP vs. inverse temperature $(K)^{-1}$ of polyol- and water-plasticised pullulan/ corn starch blends

Temperature (°C)	Gelatinised starch (%)	Pullulan (%)	Sorbitol (%)	Water (%)	O_2 ($cm^2\ s^{-1}\ Pa^{-1}$)	CO_2 ($cm^2\ s^{-1}\ Pa^{-1}$)	T_g (°C)
41.5	45	45	10	5.0	$5.92(\pm 0.82) \times 10^{-16}$	$9.82(\pm 0.85) \times 10^{-16}$	60.5 ± 1.2
62.6	45	45	10	5.0	$6.42(\pm 0.70) \times 10^{-15}$	$9.56(\pm 0.48) \times 10^{-15}$	
84.1	45	45	10	5.0	$7.85(\pm 0.90) \times 10^{-14}$	$1.58(\pm 0.60) \times 10^{-13}$	
22.9	45	45	10	10.0	$4.15(\pm 0.55) \times 10^{-15}$	$8.86(\pm 0.72) \times 10^{-15}$	38.2 ± 1.8
42.5	45	45	10	10.0	$3.55(\pm 0.90) \times 10^{-14}$	$1.09(\pm 0.20) \times 10^{-13}$	
64.8	45	45	10	10.0	$9.61(\pm 0.89) \times 10^{-13}$	$4.20(\pm 0.55) \times 10^{-12}$	
40.5	40	40	20	3.3	$4.23(\pm 0.56) \times 10^{-15}$	$7.32(\pm 0.56) \times 10^{-15}$	57.8 ± 2.1
60.3	40	40	20	3.3	$7.74(\pm 0.68) \times 10^{-15}$	$1.89(\pm 0.55) \times 10^{-14}$	
82.9	40	40	20	3.3	$7.32(\pm 0.65) \times 10^{-14}$	$1.21(\pm 0.15) \times 10^{-13}$	
19.4	40	40	20	6.0	$2.31(\pm 0.40) \times 10^{-14}$	$5.85(\pm 0.60) \times 10^{-14}$	39.4 ± 1.0
41.5	40	40	20	6.0	$6.61(\pm 0.54) \times 10^{-14}$	$1.13(\pm 0.24) \times 10^{-13}$	
63.7	40	40	20	6.0	$5.34(\pm 0.60) \times 10^{-13}$	$9.75(\pm 0.81) \times 10^{-13}$	
			Xylose				
48.5	45	45	10	5.0	$1.03(\pm 0.14) \times 10^{-15}$	$4.69(\pm 0.73) \times 10^{-15}$	69.0 ± 1.4
73.0	45	45	10	5.0	$3.49(\pm 0.70) \times 10^{-15}$	$9.05(\pm 0.37) \times 10^{-15}$	
96.0	45	45	10	5.0	$1.42(\pm 0.35) \times 10^{-14}$	$6.39(\pm 0.84) \times 10^{-14}$	
28.2	45	45	10	7.5	$9.44(\pm 0.83) \times 10^{-15}$	$2.97(\pm 0.65) \times 10^{-14}$	52.5 ± 1.3
52.7	45	45	10	7.5	$2.73(\pm 0.34) \times 10^{-14}$	$5.60(\pm 0.54) \times 10^{-14}$	
75.4	45	45	10	7.5	$9.85(\pm 0.83) \times 10^{-14}$	$3.32(\pm 0.36) \times 10^{-13}$	
36.6	40	40	20	5.0	$2.57(\pm 0.80) \times 10^{-15}$	$2.84(\pm 0.43) \times 10^{-15}$	59.0 ± 1.7
55.9	40	40	20	5.0	$3.74(\pm 0.49) \times 10^{-15}$	$7.35(\pm 0.81) \times 10^{-15}$	
77.9	40	40	20	5.0	$9.84(\pm 0.81) \times 10^{-15}$	$2.82(\pm 0.60) \times 10^{-14}$	
9.5	40	40	20	8.0	$4.43(\pm 0.72) \times 10^{-14}$	$6.10(\pm 0.47) \times 10^{-14}$	27.1 ± 1.2
31.0	40	40	20	8.0	$7.90(\pm 0.65) \times 10^{-14}$	$1.22(\pm 0.20) \times 10^{-13}$	
54.9	40	40	20	8.0	$6.75(\pm 0.80) \times 10^{-13}$	$1.72(\pm 0.57) \times 10^{-12}$	

crystallinity, high chain-to-chain packing, a degree of polarity and a high T_g (McHugh & Krochta, 1994; Robertson, 1993). In attempting to characterise and model edible film permeability properties, further complications arise from interactions between permeant and polymer as well as from temperature, relative humidity and plasticisation effects. Thus, GP modelling using an empirical approach, known as the 'group contribution theory' (Salame, 1986), has revealed large discrepancies between predicted and experimental values for water- and polyol-plasticised hydrocolloid films (Arvanitoyannis et al., 1996). This divergence was attributed to accessibility of polar (–OH) groups,

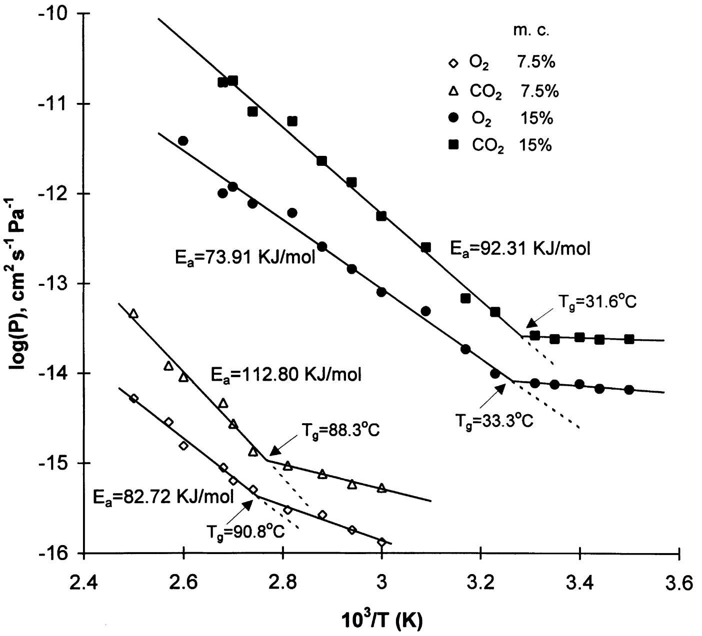

Fig. 12. Arrhenius plots for GP data (O_2 and CO_2) for films of the ps blend.

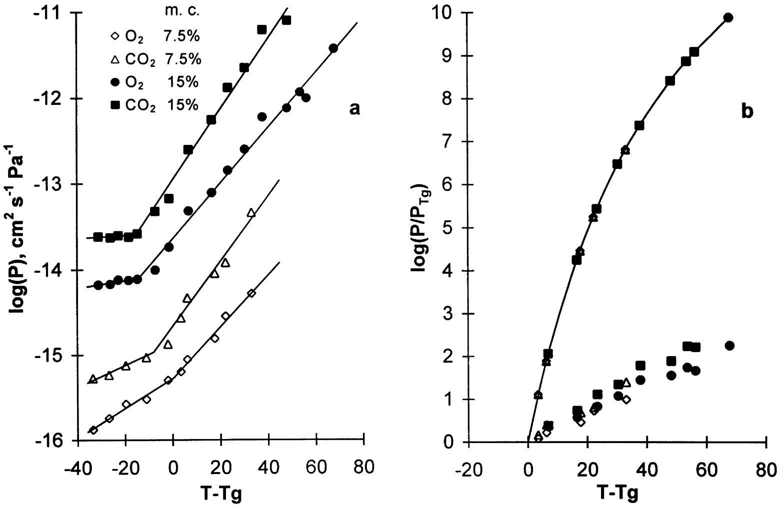

Fig. 13. Plots of permeability data (of Fig. 12) against $T - T_g$. The solid line in the (b) diagram is the theoretical curve of the WLF relationship with $C_1 = 17.44$ and $C_2 = 51.6$.

geometry of voids in the plasticised polymer, relative strength of water–water and water–polyol vs. polymer–water and polymer–polyol interactions, localised mechanical yielding of the polymer matrix and other microstructural defects (Mueller-Plathe, 1991a,b, 1992; van Krevelen, 1990; Brown, 1993). The O_2 and CO_2 permeability data of all ps blends (Table 4) showed increases in GP with the polyol level or water content, confirming previous findings on other starch-based hydrocolloid films (Arvanitoyannis et al., 1996; Arvanitoyannis & Biliaderis, 1998; Psomiadou et al., 1996). The addition of polyols and water in the ps blends increases the free volume (lowers the T_g) and thereby enhances the diffusion and permeability of gases as has been shown for various synthetic (Maeda & Paul, 1987) and natural (Butler, Vergano, Testin, & Bunn, 1996; Lieberman & Gilbert, 1973; Park & Chinnan, 1995) polymers. Using data compiled by McHugh and Krochta (1994) and Guilbert, Gontard, and Gorris (1996), the O_2 permeability values of Table 4 are comparable to those of other biopolymer films (2.7×10^{-15} cm^2 s^{-1} Pa^{-1} for collagen, 23°C/63% RH; 11.2×10^{-15} cm^2 s^{-1} Pa^{-1} for methylcellulose, 24°C/50% RH; 16.7×10^{-15} cm^2 s^{-1} Pa^{-1} for whey protein/sorbitol 1.5/1, 23°C/75% RH; 3.79×10^{-15} cm^2 s^{-1} Pa^{-1} for pullulan, 25°C/30% RH) and much lower than the permeabilities of LDPE (217×10^{-15} cm^2 s^{-1} Pa^{-1}, 23°C/50% RH) and HDPE (49×10^{-15} cm^2 s^{-1} Pa^{-1}, 23°C/50% RH).

The GP also increased with temperature. For gases and vapours, the temperature dependence of permeability often obeys the Arrhenius relationship

$$P = P_0 \exp(-E_P/RT),$$

where P_0 is a constant (a kinetic frequency factor), R is the gas constant, and E_P is the activation energy for permeation. Thus, Arrhenius plots have been used to describe the exponential variation of permeability, diffusivity, and solubility coefficients with temperature (Doyon, Gagnon, Toupin, & Castaigne, 1991; Eichler & Miltz, 1993; Pascat, 1985). Fig. 12 shows Arrhenius plots for O_2 and CO_2 permeability in ps at two levels of water content. These plots also illustrate how an indirect determination of the glass transition temperature can be made from GP data. Specifically, a change in slope is observed at the glass transition zone for the permeability implying discretely different activation energies in the rubbery vs. the glassy state. This behaviour is a manifestation of changes in segmental mobility of the polymer chains upon traversing T_g. From the slopes of the linear segments of the Arrhenius plots it appears that the activation energies in the rubbery state are much larger than those of the glassy state. This observation is not unusual, as has been shown for the temperature dependence of gas diffusion and permeability coefficients in polyvinyl acetate (Meares, 1954), polyethylene terephthalate (Michaels, Vieth, & Barrie, 1963a,b) and polypropylene (Brandt, 1959). Meares (1954, 1957) proposed the following idealised concept for the gas diffusion processes in polymers to explain the differences in apparent activation energies in the two temperature regimes. At temperatures above T_g, gas molecules which dissolve in the polymer must create their own 'holes' by separating interchain polymer contacts. The permeant then diffuses through the polymer matrix along cylindrical voids created by the synchronised rotation of polymer chain segments. Below T_g, the matrix consists of regions with densely packed chains (having limited freedom of rotation) and less compact regions with 'holes' into which the permeant molecules adsorb. In the latter case, the gas molecules can pass through these 'holes' by a slight compression of localised chains in the dense regions. This localised compression in the glassy state does not create the long cavities common in the rubbery state; i.e. the zone of chain activation is much larger in the rubbery state due to increased segmental mobility above T_g. This postulate was

Table 5
WVP (25°C) of pullulan/corn starch films

Sample	WVTR (g/m s Pa)
ps	$1.92(\pm 0.17) \times 10^{-10}$
ps/s10	$3.17(\pm 0.37) \times 10^{-10}$
ps/s20	$3.48(\pm 0.46) \times 10^{-10}$
ps/x10	$4.07(\pm 0.39) \times 10^{-10}$
ps/x20	$4.88(\pm 0.58) \times 10^{-10}$

further supported by the findings of Michaels et al. (1963a,b) on polyethylene terephthalate.

For diffusion and relaxation events in the rubbery state, the WLF equation has been suggested as a more appropriate kinetic model, than the Arrhenius equation, to describe the temperature dependence of various translational diffusion-limited and mechanical/structural relaxation processes (Levine & Slade, 1992; Slade & Levine, 1991, 1993). The GP data were thus fitted to the WLF model (Fig. 13) to test its applicability at temperatures above the T_g. Although very good fits ($r^2 > 0.96$) were obtained between log P and $T - T_g$ for all four data sets (Fig. 13(a)), there was a clear indication that GP changes with increasing temperature do not follow the WLF model with the fixed 'universal coefficients', $C_1 = 17.44$ and $C_2 = 51.6$ (Williams et al., 1955). As can be seen from Fig. 13(b), the curves constructed with the measured permeability values for O_2 and CO_2 are not as steep as the WLF master curve in the same temperature range. The calculated values (best fitting) for the WLF coefficients varied for C_1 between 3.1 and 6.0, while for C_2 between 58.8 and 103.4 K. Thus, the WLF equation with fixed coefficients cannot be assumed as a valid model to predict GP in the rubbery domain of these water-plasticised biopolymer blends. Simatos and Blond (1991) have reached similar conclusions in analysing various literature reports on kinetic data of deteriorative chemical and enzymic reactions in the frozen state; the reaction kinetics could not be described by the WLF model, using T_g as a reference temperature and taking as numerical values for C_1 and C_2,17.44 and 51.6, respectively. Peleg (1992) has also showed that for a variety of polymers and amorphous sugars, the magnitude of C_1 and C_2 may vary considerably from the 'universal constants' depending on the material, the measured property and the selected reference temperature.

Accurate measurements of WV barrier properties of hydrocolloid films is by far a more difficult task than for most other gas permeants. Hydrophilic films exposed to water vapour partial pressure gradients are non-homogeneous due to the presence of varying amounts of water within different film regions. The water sorption isotherms of hydrophilic polymer films are highly non-linear (Fig. 1), and their diffusivities are strongly dependent on the water content of the film. At high RHs 'clustering' of water molecules occurs in their diffusion through microcavities and this leads to increases in free-volume and in polymer permeability (McHugh & Krochta, 1994; Schult & Paul, 1996). The WVP data are thus used for comparative purposes under the selected test conditions. Table 5 shows that increasing levels of sorbitol or xylose in the blends led to higher WVP. The effect of polyols may be attributed to their plasticising action (greater interchain distances), the promotion of water clustering by competing with water at active sites of the polymer matrix and the formation of microcavities (lesions) in the film structure (Lieberman & Gilbert, 1973; Lieberman, Gilbert, & Srinivasa, 1972; Park & Chinnan, 1995). Enhancement of WVP by polyols has also been reported for other biopolymer films (Arvanitoyannis et al., 1996; Arvanitoyannis & Biliaderis, 1998; Park & Chinnan, 1995).

Acknowledgements

This study has been carried out with financial support from the Commission of the European Communities, Agriculture and Fisheries (FAIR) specific RTD programme CT96-1085 “Enhancement of Quality of Food and Related Systems by Control of Molecular Mobility”. It does not necessarily reflect its views and in no way anticipates the Commission’s future policy in this area.

References

Angell, C. A., Bressel, R. D., Green, J. L., Kanno, H., Oguni, M., & Sare, E. J. (1994). *J. Food Engng, 22*, 115–142.

Appelqvist, I. A. M., Cooke, D., Gidley, M., & Lane, S. J. (1993). *Carbohydr. Polym., 20*, 291–299.

Arvanitoyannis, I., & Biliaderis, C. G. (1998). *Food Chem., 62*, 333–342.

Arvanitoyannis, I., Kalichevsky, M. T., Blanshard, J. H. V., & Psomiadou, E. (1994). *Carbohydr. Polym., 24*, 1–15.

Arvanitoyannis, I., & Psomiadou, E. (1994). *J. Appl. Polym. Sci., 51*, 1863–1899.

Arvanitoyannis, I., Psomiadou, E., & Nakayama, A. (1996). *Carbohydr. Polym., 31*, 179–192.

ASTM (1966). Annual Book of ASTM standards, D 1434-66. American Society for Testing and Materials. Philadelphia, USA.

ASTM (1989). Annual Book of ASTM standards, D 828-88. American Society for Testing and Materials. Philadelphia, USA.

Attenburrow, G. E., Davies, A. P., Goodband, R. M., & Ingman, S. J. (1992). *J. Cereal Sci., 16*, 1–12.

Bader, H. G., & Goritz, D. (1994). *Starch, 46*, 435–439.

Berens, A. R., & Hodge, I. M. (1982). *Macromolecules, 15*, 756–761.

Biliaderis, C. G. (1998). In R. H. Walter (Ed.), *Polysaccharide Association Structures in Food*, (pp. 57). New York: Marcel Dekker.

Biliaderis, C. G., Page, C. M., Maurice, T. J., & Juliano, B. M. (1986). *J. Agr. Food Chem., 34*, 6–14.

Bizot, H. (1983). In R. Jowitt & F. Escher & B. Hallstrom & H. F. Th. Meffert & W. E. L. Spiess & G. Vos (Eds.), *Physical properties of foods*, (pp. 43). London: Applied science.

Bizot, H., Le Bail, P., Leroux, B., Davy, J., Roger, P., & Buleon, A. (1997). *Carbohydr. Polym., 32*, 33–50.

Brandt, W. W. (1959). *J. Polym. Sci., 16*, 415–423.

Brown, D. J. (1993). In J. M. V. Blanshard & P. J. Lillford (Eds.), *The Glassy State in Foods*, (pp. 453). Loughborough, UK: Nottingham University Press.

Brunauer, S., Emmett, P. H., & Teller, E. (1938). *J. Am. Chem. Soc.*, *60*, 309–319.

Buera, M. P., Jouppila, K., Roos, Y. H., & Chirife, J. (1998). *Cereal Chem.*, *75*, 64–69.

Butler, B. L., Vergano, P. J., Testin, R. F., Bunn, J. M., & Wiles, J. L. (1996). *J. Food Sci.*, *61*, 953–955, 961.

Cherian, G., Gennadios, A., Weller, C., & Chinachoti, P. (1995). *Cereal Chem.*, *72*, 1–6.

Couchman, P. R., & Karasz, F. E. (1978). *Macromolecules*, *11*, 117–119.

Donald, A. M., Warburton, S. C., & Smith, A. C. (1993). In J. M. V. Blanshard & P. J. Lillford (Eds.), *The Glassy State in Foods*, (pp. 375). Loughborough, UK: Nottingham University Press.

Doyon, G., Gagnon, J., Toupin, C., & Castaigne, F. (1991). *Packag. Technol. Sci.*, *4*, 157–165.

Eichler, S., & Miltz, J. (1993). *J. Appl. Polym. Sci.*, *50*, 2095–2098.

Fennema, O. R. (1996). In O. R. Fennema (Ed.), *Food Chemistry*, 3rd. (pp. 17). New York: Marcel Dekker.

Ferry, J. D. (1980). Viscoelastic properties of polymers. 3rd. New York: Wiley.

Fontanet, I., Davidou, S., Dacremont, C., & Le Meste, M. (1997). *J. Cereal Sci.*, *25*, 303–311.

Forssell, P. M., Mikkila, J., Moates, G. K., & Parker, R. (1997). *Carbohydr. Polym.*, *34*, 275–282.

Georget, D. M. R., & Smith, A. C. (1995). *Cereal Chem.*, *28*, 305–311.

Gidley, M. J., Cooke, D., & Ward-Smith, S. (1993). In J. M. V. Blanshard & P. J. Lillford (Eds.), *The glassy state in foods*, (pp. 303). Loughborough, UK: Nottingham University Press.

Gontard, N., Guilbert, S., & Cuq, J. -L. (1993). *J. Food Sci.*, *58*, 206–211.

Gontard, N., & Ring, S. (1996). *J. Agric. Food Chem.*, *44*, 3474–3478.

Gordon, M., & Taylor, J. S. (1952). *J. Appl. Chem.*, *2*, 493–500.

Greenspan, L. (1977). *J. Res. Natl. Bur. Stand. Sect. A*, *81A*, 89–96.

Guilbert, S., Gontard, N., & Gorris, L. G. M. (1996). *Lebensm.-Wiss. u.-Technol.*, *29*, 10–17.

Hallberg, L. M., & Chinachoti, P. (1992). *J. Food Sci.*, *57*, 1201–1204 see also p. 1299.

Harris, M., & Peleg, M. (1996). *Cereal Chem.*, *73*, 225–231.

Hartley, L., Chevance, F., Hill, S. E., Mitchell, J. R., & Blanshard, J. M. V. (1995). *Carbohydr. Polym.*, *28*, 83–89.

Hatley, R. H. M., & Mant, A. (1993). *Int. J. Biol. Macromol.*, *15*, 227–232.

Hodge, I. M., & Berens, A. R. (1982). *Macromolecules*, *15*, 762–770.

Hoseney, R. C., Zeleznak, K., & Lai, C. S. (1986). *Cereal Chem.*, *63*, 285–286.

Ibar, J. P. (1997). *J. Macromol. Sci., Rev. Macromol. Chem. Phys.*, *C37* (3), 389–458.

Jouppila, K., & Roos, Y. H. (1994). *J. Dairy Sci.*, *77*, 1798–1808.

Kaletunc, G., & Breslauer, K. J. (1993). *Cereal Chem.*, *70*, 548–552.

Kalichevsky, M. T., & Blanshard, J. M. V. (1992). *Carbohydr. Polym.*, *19*, 271–278.

Kalichevsky, M. T., & Blanshard, J. M. V. (1993). *Carbohydr. Polym.*, *20*, 107–113.

Kalichevsky, M. T., Blanshard, J. M. V., & Tokarczuk, P. F. (1993b). *Int. J. Food Sci. Technol.*, *28*, 139–151.

Kalichevsky, M. T., Jaroszkiewicz, E. M., Ablett, S., Blanshard, J. M. V., & Lillford, P. J. (1992a). *Carbohydr. Polym.*, *18*, 77–88.

Kalichevsky, M. T., Jaroszkiewicz, E. M., & Blanshard, J. M. V. (1992b). *Int. J. Biol. Macromol.*, *14*, 257–266.

Kalichevsky, M. T., Jaroszkiewicz, E. M., & Blanshard, J. M. V. (1992c). *Int. J. Biol. Macromol.*, *14*, 267–273.

Kalichevsky, M. T., Jaroszkiewicz, E. M., & Blanshard, J. M. V. (1993a). *Polymer*, *34*, 346–347.

Kalichevsky, M. T., Orford, P. D., & Ring, S. G. (1986). *Carbohydr. Polym.*, *6*, 145–154.

Kalichevsky, M. T., & Ring, S. G. (1987). *Carbohydr. Res.*, *162*, 323–328.

Kaminski, W., & Al-Bezweni, M. (1994). *Int. J. Food Sci. Technol.*, *29*, 129–136.

Karel, M., Buera, M. P., & Roos, Y. (1993). In J. M. V. Blanshard & P. J. Lillford (Eds.), *The glassy state in foods*, (pp. 13). Loughborough, UK: Nottingham University Press.

Keinath, S. E., Miller, R. L., & Rieke, J. K. (1987). Order in the amorphous state of polymers. New York: Plenum Press.

Kelley, S. S., Rials, T. G., & Glasser, W. G. (1987). *J. Mater. Sci.*, *22*, 617–624.

Kirby, A. R., Clark, S. A., Parker, R., & Smith, A. C. (1993). *J. Mater. Sci.*, *28*, 5937–5942.

Labuza, T. P., Kaanane, A., & Chen, J. Y. (1985). *J. Food Sci.*, *50*, 385–391.

Lawton, J. W. (1996). *Carbohydr. Polym.*, *29*, 203–208.

Le Meste, M., Huang, V. T., Panama, J., Anderson, G., & Lentz, R. (1992). *Cereal Foods World*, *37*, 264–267.

Le Meste, M., Roudaut, G., & Davidou, S. (1996). *J. Thermal Anal.*, *47*, 1361–1375.

Levine, H., & Slade, L. (1988a). In J. R. Mitchell & J. M. V. Blanshard (Eds.), *In Food Structure: its creation and evaluation*, (pp. 149). London: Butterworths.

Levine, H., & Slade, L. (1988b). *Cryo-Letters*, *9*, 21–63.

Levine, H., & Slade, L. (1992). In H. G. Schwartzberg & R. W. Hartel (Eds.), *Physical Chemistry of Foods*, (pp. 83). New York: Marcel Dekker.

Lieberman, E. R., & Gilbert, S. G. (1973). *J. Polym. Sci.*, *41*, 33–43.

Lieberman, E. R., Gilbert, S. G., & Srinivasa, V. (1972). *N.Y. Acad. Sci. II.*, *34*, 694–708.

Lillie, M. A., & Gosline, J. M. (1993). In J. M. V. Blanshard & P. J. Lillford (Eds.), *The glassy state in foods*, (pp. 281). Loughborough, UK: Nottingham University Press.

Livings, S. J., Breach, C., Donald, A. M., & Smith, A. C. (1997). *Carbohydr. Polym.*, *34*, 347–355.

Lourdin, D., Della Valle, G., & Colonna, P. (1995). *Carbohydr. Polym.*, *27*, 261–270.

Blanshard, J. M. V. & Lillford, P. J. (Eds.). (1993). The glassy state in foods (pp. 223). Loughborough, UK: Nottingham University Press.

Maeda, Y., & Paul, D. R. (1987). *J. Polym. Sci., Polym. Phys. Ed.*, *25*, 1005–1016.

Mansfield, M. L. (1993). In J. M. V. Blanshard & P. J. Lillford (Eds.), *The glassy state in foods*, (pp. 103). Loughborough, UK: Nottingham University Press.

Martin-Polo, M., Voilley, A., Blond, G., Colas, B., Mesnier, M., & Floquet, N. (1992). *J. Agric. Food Chem.*, *40*, 413–418.

McHugh, T. H., & Krochta, J. M. (1994). In J. M. Krochta & E. A. Baldwin & M. O. Nisperos-Carriedo (Eds.), *Edible coatings and films to improve food quality*, (pp. 139). Technomic.

Meares, P. (1954). *J. Am. Chem. Soc.*, *76*, 3415–3422.

Meares, P. (1957). *Trans. Faraday Soc.*, *53*, 101–106.

Michaels, A., Vieth, W., & Barrie, J. (1963a). *J. Appl. Phys.*, *34*, 1–12.

Michaels, A., Vieth, W., & Barrie, J. (1963b). *J. Appl. Phys.*, *34*, 13–20.

Mueller-Plathe, F. (1991a). *J. Chem. Phys.*, *94*, 3129–3199.

Mueller-Plathe, F. (1991b). *Macromolecules*, *24*, 6475–6476.

Mueller-Plathe, F. (1992). *J. Chem. Phys.*, *96*, 3200–3205.

Nakamura, S., & Tobolsky, A. V. (1967). *J. Appl. Pol. Sci.*, *11*, 1371–1386.

Nicholls, R. J., Appelqvist, I. A. M., Davies, A. P., Ingman, S. J., & Lillford, P. J. (1995). *J. Cereal Sci.*, *21*, 25–36.

Noel, T. R., Parker, R., Ring, S. G., & Tatham, A. S. (1995). *Int. J. Biol. Macromol.*, *17*, 81–85.

Olabisi, O., Robeson, L. M., & Shaw, M. T. (1979). Polymer–polymer miscibility. New York: Academic Press.

Ollett, A. -L., Parker, R., & Smith, A. C. (1991). *J. Mater. Sci.*, *26*, 1351–1356.

Orford, P. D., Parker, R., Ring, S. G., & Smith, A. C. (1989). *Int. J. Biol. Macromol.*, *11*, 91–96.

Park, H. J., & Chinnan, M. S. (1995). *J. Food Engng*, *25*, 497–507.

Pascat, B. (1985). In J. Comyn (Ed.), *Polymer permeability*, (pp. 7). New York: Elsevier Applied Science.

Peleg, M. (1992). *Crit. Rev. Food Sci. Nutr.*, *32*, 59–66.

Peleg, M. (1996a). *Crit. Rev. Food Sci. Nutr.*, *36*, 49–67.

Peleg, M. (1996b). *Cereal Chem.*, *73*, 712–715.

Platzer, N.A.J. (1965). Plasticisation and plasticiser processes. Adv. Chem. Ser. 48 ACS. Washington, D.C.

Psomiadou, E., Arvanitoyannis, I., & Yamamoto, Y. (1996). *Carbohydr. Polym.*, *31*, 193–204.

Rahman, S. (1995). Food Properties Handbook. Boca Raton, FL: CRC Press.

Rindlav, A., Hulleman, S. H. D., & Gatenholm, P. (1997). *Carbohydr. Polym.*, *34*, 25–30.

Robertson, G. L. (1993). In G. L. Robertson (Ed.), *Food packaging: principles and practice*, (pp. 73). New York: Marcel Dekker.

Rockland, L. B. (1960). *Anal. Chem.*, *32*, 1375–1376.

Roos, Y. H. (1995). Phase transitions in foods. New York: Academic Press.

Roos, Y. H., & Karel, M. (1991). *Food Technol.*, *26* (12), 68–71, 107.

Roos, Y. H., Karel, M., & Kokini, J. L. (1996). *Food Technol.*, *31* (11), 95–108.

Roudaut, G. (1998) Mobilité moléculaire dans des verres de produits céréaliers de cuisson: incidence sur la texture, PhD thesis, Univ. de Bourgogne, ENSBANA, Dijon, France.

Salame, M. (1986). *Polym. Engng Sci.*, *26*, 1543–1546.

Schult, K. A., & Paul, D. R. (1996). *J. Appl. Polym. Sci.*, *61*, 1865–1876.

Shogren, R. L. (1992). *Carbohydr. Polym.*, *19*, 83–90.

Simatos, D., & Blond, G. (1991). In H. Levine & L. Slade (Eds.), *Water relationships in foods*, (pp. 139). New York: Plenum Press.

Simatos, D., Blond, G., & Perez, J. (1995). In V. Barbosa-Canovas & L. Welti-Chanes (Eds.), *Food preservation by moisture control*, Lancaster, USA: Technomic.

Slade, L., & Levine, H. (1991). *Crit. Rev. Food Sci. Nutr.*, *30*, 115–360.

Slade, L., & Levine, H. (1993). In J. M. V. Blanshard & P. J. Lillford (Eds.), *The glassy state in foods*, (pp. 35). Loughborough, UK: Nottingham University Press.

Soest, J. J. G.van, Hulleman, S. H. D., Wit, D.de, & Vliegenthart, J. F. G. (1996a). *Carbohydr. Polym.*, *29*, 225–232.

Soest, J. J. G.van, Wit, D.de, & Vliegenthart, J. F. G. (1996b). *J. Appl. Polym. Sci.*, *61*, 1927–1937.

Sperling, L. H. (1986). Introduction to physical polymer science. New York: Wiley.

Sugisaki, M., Suga, H., & Seki, S. (1968). *Bull. Chem. Soc. Jpn.*, *41*, 2591–2599.

Thiewes, H. J., & Steeneken, P. A. M. (1997). *Carbohydr. Polym.*, *32*, 123–130.

van den Berg, C., & Bruin, S. (1981). In L. B. Rockland & G. F. Stewart (Eds.), *Water activity: influences on food quality*, (pp. 1). New York: Academic Press.

van Krevelen, D. W. (1990). Properties of polymers. 3rd. Amsterdam, NL: Elsevier.

Vodovotz, Y., & Chinachoti, P. (1996). *J. Food Sci.* , *61*, 932–937, 941.

Weisser, H., & Liebenspacher, F. (1989). In R. S. Singh (Ed.), *Food properties and computer-aided engineering of food processing systems*, (pp. 223). *NATO ASI Series E 168*New York: Kluwer.

Whistler, R. L., BeMiller, J. N., & Paschall, E. F. (1984). Starch: chemistry and technology. New York: Academic Press.

Williams, M. L., Landel, R. F., & Ferry, J. D. (1955). *J. Amer. Chem. Soc.*, *77*, 3701–3707.

Wurzburg, O. B. (1986). Modified starches: properties and uses. Boca Raton, FL: CRC Press.

Yuan, R., & Thompson, D. (1994). *Carbohydr. Polym.*, *25*, 1–6.

Yuen, S. (1974). *Proc. Biochem., (Nov.) 22*, 7–9.

Zeleznak, K. J., & Hoseney, R. C. (1987). *Cereal Chem.*, *64*, 121–124.